Back analysis of a building collapse under ~~snow and rain~~ snow-and-rain loads in Mediterranean area

Isabelle Ousset[1], Guillaume Evin[1], Damien Raynaud[1], and Thierry Faug[1]

[1]Univ. Grenoble Alpes, CNRS, INRAE, IRD, Grenoble INP*, IGE, 38000 Grenoble, France. *Institute of Engineering and Management Univ. Grenoble Alpes.

Correspondence: Isabelle Ousset (isabelle.ousset@inrae.fr)

Abstract. At the end of February 2018 the Mediterranean area of Montpellier in France was struck by a significant snowfall that turned into an intense rain event caused by an exceptional atmospheric situation. This rain-on-snow event produced pronounced damage to many buildings of different types. In this study, we report a detailed back analysis of the roof collapse of a large building, namely the Irstea Cévennes building. Attention is paid to the dynamics of the climatic event, on the one hand, and to the mechanical response of the metal roof structure to ~~normal loading~~different snow-and-rain loads, on the other hand. The former aspect relies on multiple sources of information that provide reliable estimates of snow heights in the area before the rain came into play and substantially modified the ~~snow quality~~load on the roof. The latter aspect relies on detailed finite element simulations of the mechanical ~~behaviour~~ behavior of the roof structure in order to assess the pressure due to ~~snow cover~~ snow-and-rain loading which could theoretically lead to failure. By combining the two approaches, it is possible to reconstruct the most probable scenario for the roof failure before its full collapse. As an example of building ~~behaviour~~ behavior and vulnerability to an ~~exceptional~~ atypical rain-on-snow event in the Mediterranean area of France, this detailed case study provides useful key points to be considered in the future for a better mitigation of such events in non-mountainous areas.

1 Introduction

In the framework of ~~snow falls~~snowfalls, there are a number of reported cases of roof collapses caused by snow loads outside mountainous areas. The following events ~~which~~ that occurred during the two past decades ~~, and are for some of them reported in the scientific literature,~~ can be mentioned:

- In France: the collapse of the roof of a warehouse at Satolas-et-Bonce in the Isère department and of a supermarket store at Bricquebec in the Manche department (January 2010), several collapses of roofs in Western France (at least nine store roofs in the Manche department) in March 2013, several damage to shops in the department of Hérault at the end of February 2018 in the cities of Béziers, Lattes, Montpellier, Peyrols (see examples shown in Figure 1).

- In Europe: the collapse of a self-weighted metallic roof in Spain in March 2004 (del Coz Díaz et al., 2012), the collapse of a public fair pavilion in Italy during February 2001 (Brencich, 2010), total collapse of the Katowice fair building in Poland which caused 65 deaths and 180 injuries in January 2006 (Biegus and Rykaluk, 2009), the collapse of the

Bad Reichenhall Ice Rink roof in Germany which led to 15 deaths the same month (Winter and Kreuzinger, 2008), the collapse of a gymnasium roof in Switzerland in 2009 (Piskoty et al., 2013), the collapse of a store hall in Gdansk (Poland) in February 2010 (Biegus and Kowal, 2013), collapse of a shopping facility in Poland during January 2015 (Krentowski et al., 2019).

- In other regions of the world: collapse of truss roof structures in Turkey in February 2003 (Caglayan and Yuksel, 2008) as well as during January and October 2015 (Piroglu and Ozakgul, 2016; Altunişik et al., 2017), many roof collapses in Northeastern United States (O'Rourke and Wikoff, 2014) during the winter 2010-2011.

The principal source of explanation given ~~for the various buildings' collapses that were induced by snow loads, and were reported in the recent above-mentioned literature , generally relies on~~ in the literature for these building collapses is a stronger (greater than the standard) snowfall hazard (Strasser, 2008; Holický and Sýkora, 2009; Geis et al., 2012; Le Roux et al., 2020). It should be noted that a poor design or insufficient material strengths may sometimes be identified as another main reason for the collapse (Biegus and Rykaluk, 2009; Caglayan and Yuksel, 2008; Brencich, 2010; del Coz Díaz et al., 2012; Biegus and Kowal, 2013; Piskoty et al., 2013; O'Rourke and Wikoff, 2014; Altunişik et al., 2017; Krentowski et al., 2019). In a large meta-analysis of building failures related to snow loads, Geis (2011) found that these incidents are commonly attributed to the large amount of snow, followed by problems in the design of the building, melting snow and rain-on-snow events.

~~Roof collapses due to heavy snowfalls occurred on 28 February and 1st March 2018 in the surroundings of Montpellier, France: collapses of (a) the shopping center Estanove in Montpellier (Photo credit: ©Jean-Michel Mart), (b) a car wash station in Lattes (Photo credit: ©Le Petit Journal de Lattes), (c) the Darty store in Peyrols (Photo credit: ©France 3 LR / S. Banus) and (d) a restaurant in La Grande Motte (Photo credit: ©France 3).~~ Roof collapses due to rain-on-snow surcharges can happen in situations where the temperature is close to 0°C during the snow event. In the United States, the potential rain-on-snow surcharge of roof snow loads has been discussed in detail by O'Rourke and Downey (2001) and is taken into account in the building standards (ASCE, 2013). Canada considers the direct sum of the snow load and the rain load (Canadian Commission on Building a . Rain-on-snow surcharges have been the subject of several studies in Japan (Otsuki et al., 2016; Takahashi et al., 2016) following a rain-on-snow event that occurred in February 2014 in the Kanto region and where the additional rain on the snow load caused the collapse of many large span structures. Using controlled outdoor experiments where rain is added to a snow cover, Otsuki et al. (2017) show that rain contributes to a larger increase of the snow load for larger roofs with smaller slope angles, due to the time it takes for the water to reach the eaves. In Europe, Eurocode 1 provides the guidelines for the calculation of the design snow load (AFNOR, 2007). Eurocode 1 specifies that in areas where rain-on-snow may cause melting followed by frost, the values of loads due to snow on the roof must be increased, especially if snow and ice can block the roof drainage system. The NF EN 1991-1-3 standard stipulates that roof snow load must be increased by 0.2 $kN.m^{-2}$ when the slope for water flow is lower than 3 %, in order to account for the snow density increase resulting from difficulties of water drainage in case of rain.

The current paper reports a detailed and specific case study of a roof collapse ~~induced by a~~ of a scientific laboratory (ex-Irstea, INRAE) which occurred on the 1st of March around 18:00 following an intense rain-on-snow ~~event which occurred in the~~

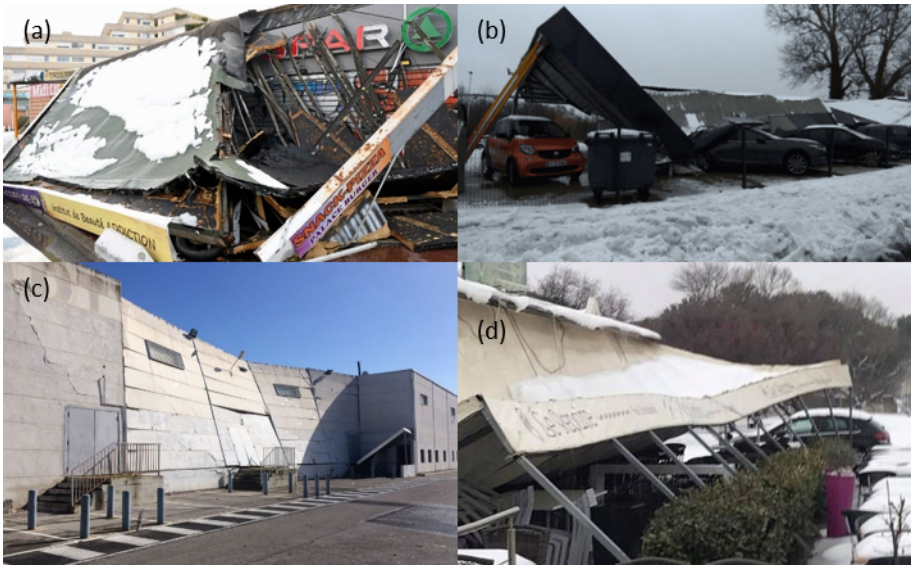

Figure 1. Roof collapses due to heavy snowfalls occurred on 28 February and 1st March 2018 in the surroundings of Montpellier, France: collapses of (a) the shopping center Estanove in Montpellier (Photo credit: ©Jean-Michel Mart), (b) a car wash station in Lattes (Photo credit: ©Le Petit Journal de Lattes), (c) the Darty store in Peyrols (Photo credit: ©France 3 LR / S. Banus) and (d) a restaurant in La Grande Motte (Photo credit: ©France 3).

~~Mediterranean area and concerned a scientific laboratory which belonged to the Irstea (now INRAE) French research institute. This is one of the several roof collapses which occurred~~ event in a Mediterranean area. Several roof collapses took place in this area ~~at the end of February 2018 (see~~ in the same period (see Figure 1).

~~Careful attention is paid to two important questions which are tackled independently in a first step: what was the maximum load admissible by the building before the event? And what was the maximum load exerted by the snow cover on the roof at the moment of the roof collapse? The first question is particularly delicate , especially because of the highly non-linear mechanical behaviour of the complex structure involved, and some uncertainty about the initial state of the structure before the event. It will be addressed in Section 3 thanks to detailed numerical simulations based on the finite element Abaqus software (Dassault Systèmes, 2017). The second question is complex too, in particular because the meteorological event consisted~~

Figure 2 shows the main damage observed during a field visit on 18 March 2018, shortly after the collapse of the experimental hall of the Irstea Cévennes building in the central part of the structure, in the east-west direction. The western and eastern facades were heavily damaged, as seen in Fig. 2a and 2c. On the contrary, the other two facades (see Figure 2b and 2d) were much less damaged due to the presence of the inner concrete walls of the offices and of the inner metal frames of the laboratory rooms along the southern and northern facades, respectively. Local damage observed on structural elements consists of (i) buckling and bending for the roof tubular profiles, (ii) bending and shear for the tubular supporting pylons and (iii) cracking on the walls of the offices (see close-up views of the damage shown in Figure S3 in the Supplementary Material (SM)).

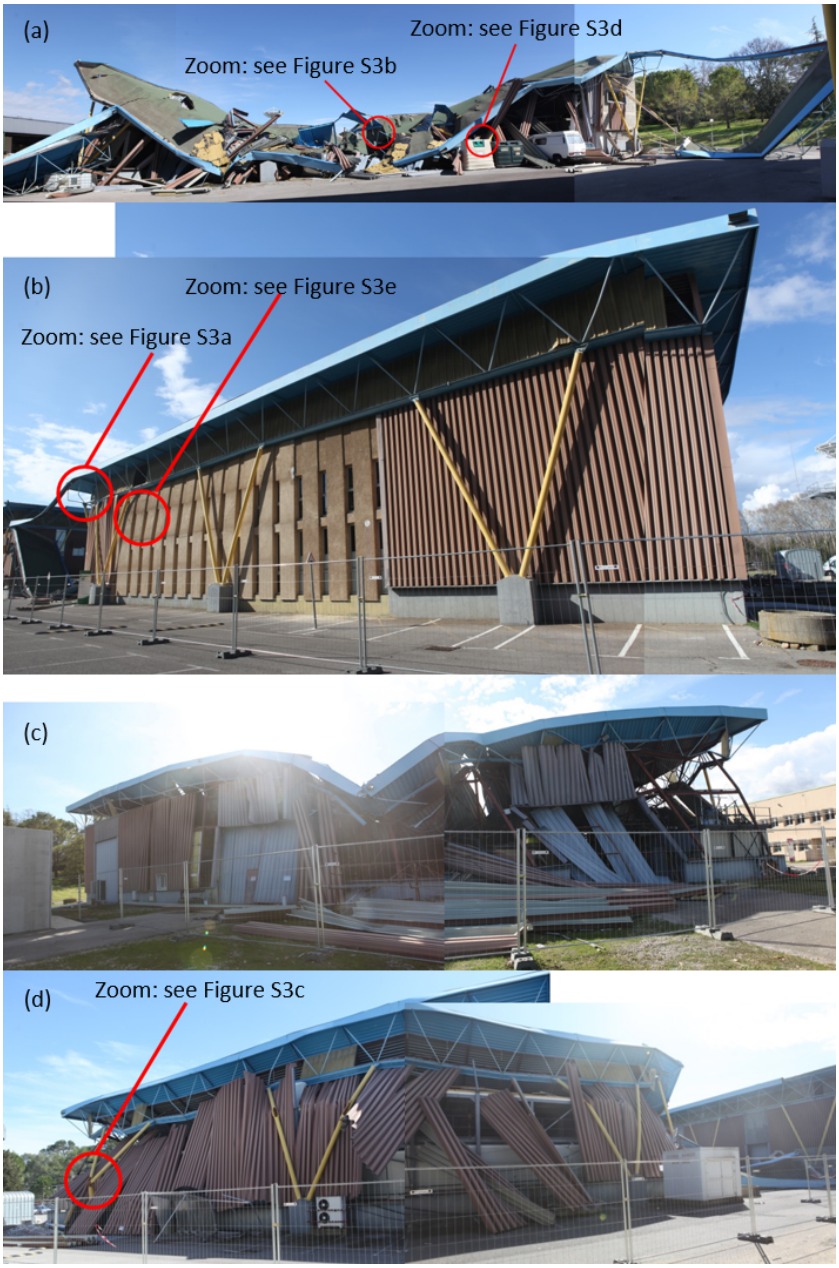

Figure 2. Different pictures showing the hierarchy of damage as observed on 18 March 2018 on the western (a), southern (b), eastern (c), and northern (d) facades of the Irstea Cévennes building.

This study aims at fulfilling the two following objectives: 1) What is the most likely load at the time of the collapse and how does it compare to the characteristic values (e.g. Eurocode Snow loads)? 2) What is the most likely scenario for the roof failure, i.e. how did the structure reach a critical state which led to its collapse? We first present the meteorological event consisting of a snowfall followed by rain at the time of the roof collapse ~~. This question will be tackled in Section 2 thanks to~~ in Section 2 using multiple sources of information: outputs from the AROME numerical model, which is the French ~~fine mesh~~ fine-mesh numerical weather forecast service model, social network testimonies and weather observations. ~~In a second step, by making the link between the analysis of the snow and rain hazard (Section 2) and the modelling~~ Section 3 presents finite element simulations of the mechanical ~~behaviour~~ behavior of the building subject to ~~a uniform pressure field that roughly mimics snow-induced loading (Section 3), a detailed analysis~~ different pressure fields representing snow-and-rain loads. Section 4 makes the link between Sections 3 and 2 and presents a detailed description of the most probable scenario for the roof collapse of Irstea Cévennes building~~is proposed in Section 4~~. This example of a roof collapse caused by an intense rain-on-snow event ~~which~~ that occurred in the Mediterranean area is ~~finally used in the discussion section~~ also used to emphasize a number of questions ~~which~~ that need to be addressed in the future, in particular~~what evolution is expected about the characteristic snow loads in non-mountainous areas in a context of climate change and what~~ , what improvements can be proposed to minimize the risk of a roof collapse due to ~~snow~~ snow-and-rain loading in those areas.

2 Description of the meteorological event

2.1 An exceptional atmospheric situation

At the end of February 2018, France, and more generally Europe, was subject to wintry weather conditions. A disordered polar vortex unleashed a very cold air mass through central Europe around 24-25 Feb. Driven by a powerful anticyclone localized in Scandinavia and a sustained eastern flux, this cold spell spread over western Europe during the following days, resulting in the most intense cold spell over Europe since Feb. 2012 which is referred to as “Beast from the East”.

Figure ~~??~~ 3 presents the outputs of the high-resolution AROME model for different times and lead times. The regional AROME model assimilates various types of observations (radar, ground measurement data, radio, ~~satellites~~ satellite radiances (see Bouttier and Roulet (2008)) and must be interpreted with care. AROME outputs provide interesting information regarding the spatio-temporal dynamics of the meteorological event. Four parameters are represented: temperature at 850 hPa, temperature at 2 m, wind at 10 m, and precipitation amount accumulated in 1 hour.

This event can be described as follows:

- **28/02/2018 08:00 - Formation of a convergence zone:** On the 28th of Feb., at 8 am (local time), just before the beginning of the snow storm, temperatures are very cold over lands in the region, in altitude ($-6°$ at 850 hPa, corr. to about 1500 m) and on the ground (between $-2°$ and $6°$ at 2 m). We can observe a line of convergence on the sea, with, on the one side, cold air brought from the ~~North-East~~ northeast related to the cold spell and, on the other side, winds

from the ~~South-East~~ southeast bringing warm air. This convergence zone will generate vertical fluxes and will create this atmospheric disturbance at the origin of important snow and rain accumulations.

- **28/02/2021 14:00 - Beginning of the snowfall:** At 2 pm (local time), important precipitation amounts occur around the convergence zone, mainly along the coast but also offshore. At the ~~North-West~~ northwest of this zone (Montpellier, Béziers), despite ~~of~~ a slight and progressive increase of temperature at the ground and in altitude, the supply of cold air from the North leads to solid precipitation only.
- **28/02/2018 20:00 - Snow/rain event:** Between 8 pm and 2 am (local time), winds from South-East intensify, and precipitation amounts on Montpellier increase. AROME model shows a temporary movement of the convergence zone from the plains. Then, a ~~North-East~~ northeast flux with cold air at low altitudes leads to snow again in the surroundings of Montpellier.
- **01/03/2018 02:00 - Warming and rainfall gets stronger:** During the night between $28/02/2018$ and $01/03/2018$, warming is rising at high altitudes (from $-3°$ at 6 pm to $0°$ at 2 am at 1500 m) and rainfall becomes dominant.
- **01/03/2018 08:00 Intense rain event:** In the morning of $01/03/2018$, despite ~~of~~ the persistence of the convergence zone and cold ground temperatures, warming in altitude is too important and precipitation only falls as rain. The collapse took place at around 18:00.

2.2 An intense rain-on-snow event

This rain-on-snow event is ~~exceptional~~ atypical in the region of Montpellier considering the accumulated amount of precipitation and the amount of precipitation fallen as snow. Ground measurements indicate that snow ~~depth~~ depths of more than 25 cm have occurred only five times since the 1950s (35 cm in February 1954, 35 cm during the winter 1962-1963, 27 cm on the 14-16/01/1987, 28 cm on the 22/01/1992 and the event described here). The empirical return period of the snow event alone exceeds 10 years (five events in 70 years). What makes the rain-on-snow event ~~exceptional~~ particularly unusual is the large amount of rainfall ~~which~~ that followed the snow event. Its occurrence can be explained by the main following elements:

- the presence of very cold air at all altitudes and in particular at the low troposphere;
- the blocking of a strong convergence zone leading to an intense rain/snow event;
- the preservation of this convergence zone and cold wind supply from the ~~North-East~~ northeast around Montpellier.

~~Figure ??~~ The last column of Figure 3 presents the evolution of the type of precipitation simulated by the AROME model for 1h lead time. AROME clearly simulates an intense snow event from 28/02/2018 at 14:00 until the end of this day, followed by a rain/snow event during the night. An intense rain event ~~brings high~~ brought large amounts of liquid precipitation during the whole day of 01/03/2018.

~~Outputs of the high resolution AROME model for the type of precipitation, for 3 runs at 1h lead time (local time is indicated). Source: Meteo-France.~~

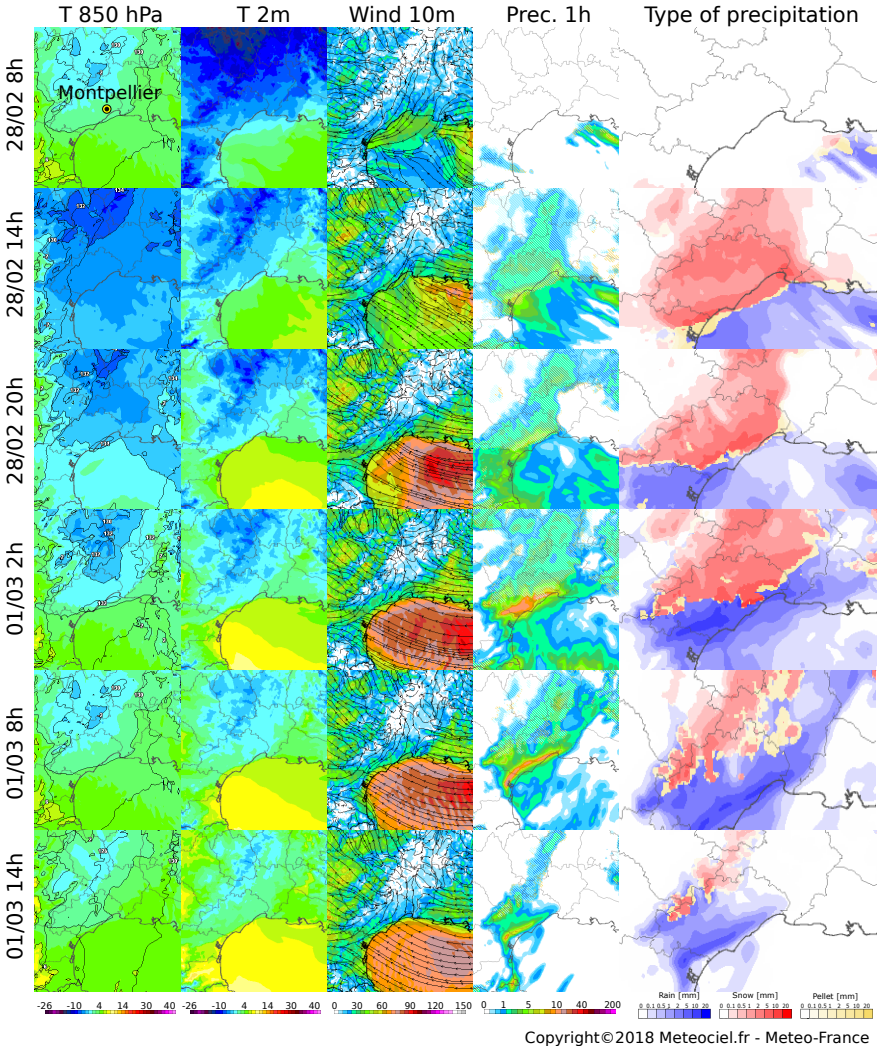

Figure 3. Outputs of the high-resolution AROME model for the following parameters: temperature at 850 hPa [°C], temperature at 2 m [°C], wind at 10 m [km/h]~~and~~ , precipitation amount accumulated in 1 hour [mm] and the corresponding type of precipitation (rain, snow or ice pellet). The maps shown on each line correspond to different runs for 1h lead time, from 28/02 at 8:00 to 01/03 at 14:00 (local time). Source: Meteo-France.

2.3 Snow accumulation

Meteo-Languedoc is an association providing various information about weather forecasts and natural risks ~~on~~ in the region around Montpellier. This exceptional data is described in ~~details~~ detail on their website~~(, last access: 24 January 2022)~~ [1] and

[1] https://www.meteolanguedoc.com/evenements-majeurs-en-languedoc-roussillon/episode-neigeux-du-28-fevrier-2018-jusqu-a-35-cm-pres-de-montpellier/p513, last access: 05 September 2023

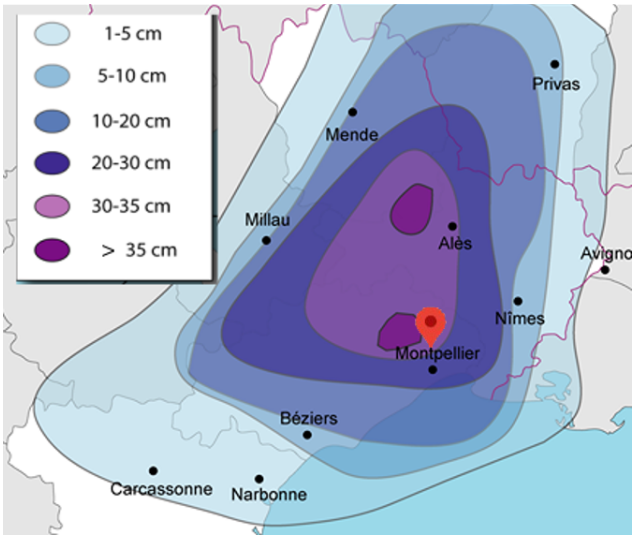

Figure 4. Snow accumulation during the snow event of 28/02/2018, based on 5000 testimonies. The red marker shows the position of the collapsed building. Source: Meteo-Languedoc.

includes various information about the meteorological event, including photos from amateurs following their ~~facebook page(, last access: 24 January 2022)~~Facebook page[2]. Through their ~~facebook~~ Facebook page, MeteoLanguedoc asked their 120 000 followers to provide observations, and photos supporting these observations. Thanks to the collection of 5 000 feedbacks, a robust estimation of the depth of the snowpack at the end of the snow event was obtained, leading to the interpolated field of snow accumulation provided in Figure 4. The data clearly shows that the snow depth was more important ~~at~~ in the North of Montpellier, likely due to a hill separating the city center from the Lavalette site.

2.4 Estimation of the snow ~~height and density~~ load at the time of the collapse

Figure 5 shows the evolution of the temperature, rain, and snow amounts according to two different and independent sources of information:

- Just next to the center of Irstea in Montpellier, a weather station (the Lavalette station) records various meteorological parameters, including temperature and rain. For this station, the tipping-bucket rain gauge is not heated and snow was probably blocking the rain gauge according to the operator of the station.
- SAFRAN reanalysis (Vidal et al., 2010) provides weather parameters at a resolution of 8 km over France, using a dense gauge network. However, this network does not include the station at Lavalette.

Both sources of information clearly show the increase ~~of~~ in temperature from the morning of 28/02/2018 until the building collapse. SAFRAN reanalysis records an accumulation of snow water equivalent of 35 mm followed by 58 mm of rainfall

[2]https://fr-fr.facebook.com/MeteoLanguedoc/, last access: 05 September 2023

before the collapse, with a rain/snow transition during the night between 28/02 and 01/03. The rain gauge, which might have underestimated the rainfall accumulation due to the presence of snow in the receptacle, records 45 mm.

The different sources of information (outputs from AROME model, social network testimonies, weather data) on the ~~snow and rain~~ snow-and-rain event lead to the following scenario. It can be considered with little uncertainty that the snow depth in the area was between 30 cm and 35 cm, on ~~a~~ cold ground. Since the Irstea building was located right next to the 30 cm curve (see Figure 4), 30 cm is considered ~~as~~ the best estimate, but there is ~~an~~ uncertainty around this estimate.

The snow ~~was having a density in the range of~~ had a density of about 250 kg.m^{-3} before the rain event, based on the fact that most of the Facebook testimonies reported a heavy snow type, which is typical of a Mediterranean area. ~~A rain-snow transition limit is then derived from available measurements, the vertical profile of temperature, and other available information. The snowpack has been filled~~ As indicated above, the snowfall has been followed by 50 to 60 mm of rainfall~~, noting that~~ . Colbeck (1977) indicates that rain can contribute up to 50% of the roof load for flat roofs with 10 m parallel flow to gutters, which corresponds closely to the specifications of the Irstea Cévennes building. Figure S5 in the ~~drainage system (see Figure ?? given in Section 3) was probably blocked by the snowpack already present on the roof at the beginning of the rain event, and that water was mostly stocked on the roof. More details on this crucial point will be given in Section 4. In light of these different sources of information and considering the additional weight provided by water from the rainfall, we can roughly estimate that the very wet snowpack~~ SM shows the roof drainage system of the Irstea Cévennes building. The roof had a slight slope of 1 % on each side of a peak line oriented north-south, which allows rainwater to flow towards the east or west of the building and drain through 20 cm high outlets located at the base of the low walls on the roof ~~easily reached a high density around 600 kg. m^{-3} at the time of the collapse, which occurred on March 1 at around 6 pm.~~

~~The ability of a snowpack to absorb water largely depends on its initial porosity and~~ edges. There were four outlets at the ends of the northern and southern edges, one in the middle of the western edge, and two at the quarter and three-quarter points of the eastern edge, as indicated by the red arrows in Figure 6a. In our case, it is likely that this drainage system was inefficient due to the combination of both (i) a small roof slope and (ii) large distances between the outlets (13 m in the north-south direction and 40 m in the ~~boundary conditions of the problem. Very loose snow, like dry and cold fresh snow (50 – 100 kg.m^{-3}), can quickly absorb a large amount of water in just afew hours. In contrast, denser snow, particularly if already wet such as the one likely involved in the event discussed in this study, may have a more limited capacity to absorb water (Marshall et al., 1999). In the former case, water will follow preferential paths and accumulate in specific areas at the bottom. Under natural conditions (open system), with constant water circulation and a homogeneous snowpack, densities higher than 300 – 400 kg. m^{-3} are not expected over a typical daily period (Marshall et al. (1999), figure 2). However, if boundary conditions prevent water evacuation (closed system) and depending on the amount of water available (intensity of the rain event until building collapse), higher ultimate densities can be expected, which correspond to an equivalent mean density for the mixture of wet snow (in some zones)and water (in other zones). In the present case, the wet snowpack was probably heterogeneous with zones of soared snow at higher density (300 – 400 kg. m^{-3}) than~~ east-west direction). Colbeck (1977) indicates that “Snow covered roof [...] would certainly collapse if a rainstorm were of sufficient duration to allow complete wetting of the unsaturated layer and full development of the saturated layer". Here, 18 hours of continuous rainfall with an average intensity of around 3 mm/h

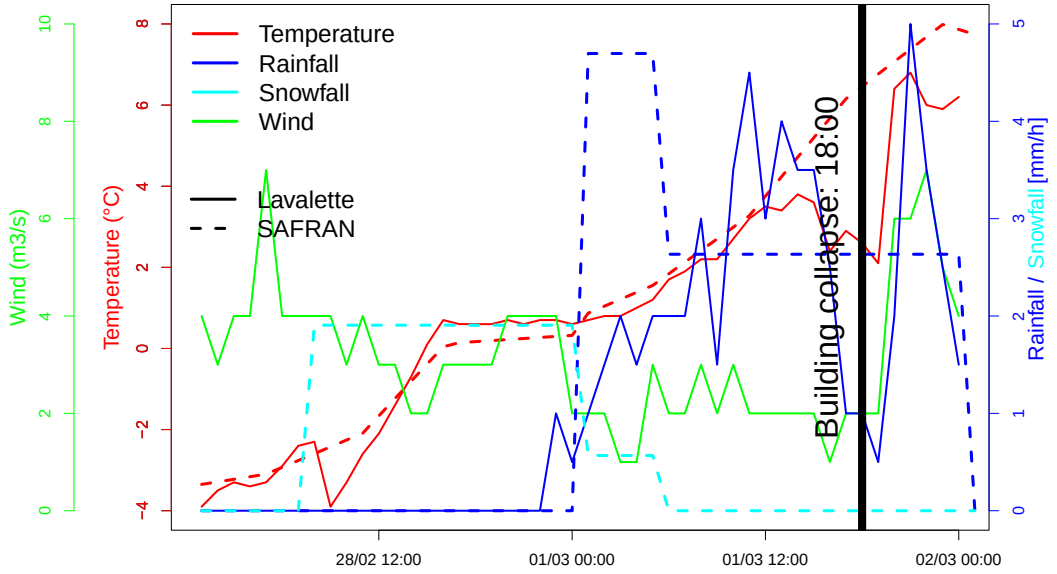

Figure 5. Weather observations at the station of Lavalette (plain lines) and SAFRAN reanalysis at the grid point covering Irstea building (dotted lines).

certainly contributed to the saturation of the snow layer. As we are not able to assess the quantity of water that could reach the outlets at the time of the collapse (which also depends on the structure deformation due to the snow load, as discussed below), it is assumed in the present analysis that the total load corresponds to the addition of the snow load and the rain load. We also assume that the initial snow ~~(250 kg.m^{-3}) and other zones at the bottom with accumulated water (1000 kg.m^{-3}) due to preferential water flows. The assumed value of 600 kg.m^{-3} used in this study for ultimate snow density corresponds to an equivalent value that defines the (equivalent) pressure exerted by the combination of snow and rain accumulations.~~

~~As the entire site was evacuated in the early afternoon of March 1, only the caretaker was present at the time of the building collapse, but he did not observe the snow~~ load (before the rain) on the roof is assumed to be equal to the snow load on the ground for several reasons. Firstly, the roof slope was low and there was a small wall around the edges of the roof. Secondly, the wind was not significant enough to modify the snow distribution on the roof. ~~Consequently, there is no information available regarding the depth and distribution of the snow on the roof. Given that the wind was only at Force 1 with a velocity between~~ Finally, the observed temperatures suggest that there was no snowmelt during the snowfall event.

In the remainder of this study, we thus assume that at the time of the collapse which occurred on March 1 ~~and 4 m~~at around 18:00, the snow-and-rain load is the outcome of 30 cm of initial snow with a density of 250 kg.m^{-3} (which corresponds to a load of about 736 N.m^{-2}) and 50 to 60 mm of rainfall (*i.e.* an additional load of $490 - 589$ N.m^{-2}). This results in a snow-and-rain load of about 1 226 to 1 325 N.m^{-2}. ~~s^{-1} during both days, it is unlikely that the wind could have had an effect on the distribution of snow on the roof and on the collapse of the building.~~

3 ~~Modelling~~ Modeling of mechanical ~~behaviour~~ behavior of the loaded building

3.1 ~~Description~~ Initial state of the building (before collapse)

3.1.1 ~~Initial state (before collapse)~~

The Cévennes building was an experimental hall built in 1982 ~~and situated at~~ on the Lavalette domain in Montpellier~~(see Figure ?? in Appendix ??)~~, in the South East of France. At the time of its failure, it ~~sheltered~~ housed a wind tunnel and a mezzanine level built in 2014 along the northern facade, ~~as well as~~ and offices on two ~~levels~~ floors along the southern facade. Figure 6 gives an overview of the Cévennes building before ~~damage. Its dimensions on the ground were 40.5~~ and after the damage. The dimensions of the roof were $l = 45$ m in the east-west direction and ~~49~~ $L = 54$ m in the north-south direction ~~(area of almost 2 000 m^2)~~ and 10 m high.

The supporting structure of the building consisted of three-dimensional vertical ~~metallic~~ metal trusses designed to support the flat roof (see ~~an example shown~~ sketches in Figure ~~??a)and themselves~~ S1 in the SM), which in turn were supported by metal tubular pylons that were arranged along the facades of the building. The lattice structure, consisting of ~~elements~~ welded or bolted ~~together~~elements, extends over the entire roof ~~surface and withstands all the forces acting upon~~ area and resists all forces acting on it. For the southern, western, and northern facades of the building, the tubular pylons consisted of two round tubular profiles arranged in a V-shape and sealed on concrete blocks anchored ~~in~~ to the ground (see photograph ~~on Figure ??b, and sketches on Figures ??a and ??b~~ in Figure 6c, sketches in Figures S1a,b in the SM and the geometric properties of the structure in Table S1 in the SM). For the ~~eastern~~ east facade of the building, they consisted of rectangular tubular profiles and a Saint Andrew's cross obtained with T-profiles (~~see sketch on Figure ??c~~Figure S1c in the SM). It ~~is worth noting here~~ should be noted that no such tubular pylons ~~had been settled~~ were placed inside the building in order to allow the movement of ~~large-size~~ large vehicles, such as agricultural tractors.

~~View of the supporting structure of the Irstea Cévennes building before its damage: (a) red-colored roof metal frame and (b) supporting tubular pylons (in yellow) along the facades.~~

~~Sketches showing the geometrical details (size and shape) of the metallic structure of every facade of the Irstea Cévennes building.~~

~~The roof had a slight slope of 1 % on each side of a peak line oriented north south, which allows rainwater to flow towards the east or west of the building and drain through 20 cm high outlets located at the base of the low walls on the roof edges, as shown in Figure ??. There were four outlets at the ends of the north and south edges, one in the middle of the west edge, and two at the quarter and three-quarter points of the east edge, as indicated by the red arrows in Figure 6.~~

~~Close-up view of the roof rain drainage system of the Irstea Cévennes building.~~

3.1.1 ~~Damage observed (after collapse)~~

~~This section gives a brief summary of the main damage observed during a field visit on 18 March 2018. Additional details are provided in Appendix ??. The snow load led to the collapse of the experimental hall of the Irstea Cévennes building in the~~

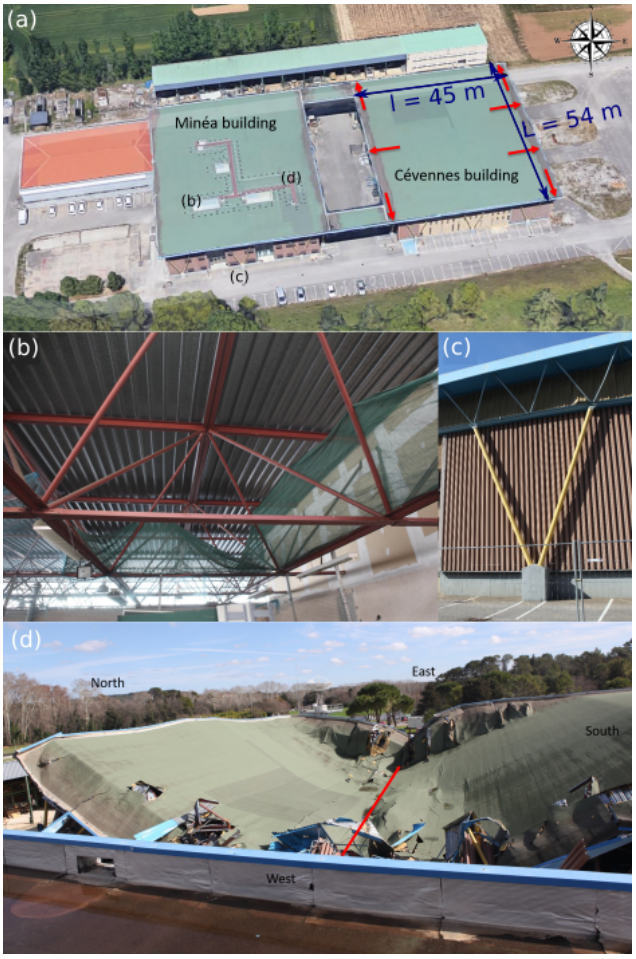

Figure 6. (a) Overview of the Irstea Cévennes building before the damage, with rainwater drainage points ~~of rainwater~~ indicated by red arrows. The dimensions of the roof are given in blue, and the height of the building is 10 m. The letters indicate where the photos of the other subplots were taken (~~Photo~~ photo credit: ©Google Earth 2014, adapted by I. Ousset). (b-c) View of the supporting structure of the Irstea Cévennes building before its damage: (b) red-coloured metal roof frame and (c) supporting tubular pylons (in yellow) along the facades. (d) Overview of the damaged Irstea Cévennes building. The red line indicates the direction perpendicular to the direction of the main deflection of the roof after the collapse.

240 ~~central part of the structure, in the west-east direction, as seen by the red line in Figure ??. The western and eastern facades were heavily damaged, as seen in Figs. 2a and 2c. On the contrary, the other two facades (see Figure 2b and 2d) were much less damaged due to the presence of the inner concrete walls of the offices and of the inner metal frames of the laboratory rooms along the south and north facades, respectively.~~

~~Overview of the damaged Irstea Cévennes building.~~

Different pictures showing the hierarchy of damage as observed on 18 March 2018 on western (a), southern (b), eastern (c) and northern (d) facades of the Irstea Cévennes building.

Local damage observed on structural elements consist in (i) buckling and bending for the roof tubular profiles, (ii) bending and shear for the tubular supporting pylons and (iii) cracking for the offices' walls. Close-up views of those damage are shown in Figure **??**.

3.2 Description of the finite element model

In order to investigate in detail the mechanical response of the Irstea Cévennes building and thus better understand its collapse under snow and rain loading, the metal supporting structure was modelled using the Finite Element (FE) Abaqus software (Dassault Systèmes, 2017). Figure **??** shows an overall sketch of the modelled structure with respect to the description of the building provided in the previous subsection. The details of the roof metal frame which was fully modelled by the FE Abaqus are shown in Figure **??**. The dimensions of the structure and of all its components are given in Table **??**.

Overview of the metal structure of the Cévennes building modelled with the FE Abaqus software.

The structure is modelled in Abaqus by 132778 Timoshenko beam elements of B31 (two-node linear beam element in space) type and 0.05 m long.

The Irstea Cévennes building dates back to the 1980s, and as such, obtaining exact design records has proven to be very difficult. The type of steel used for the supporting structure is therefore unknown, and no material testing was carried out after the collapse. It is assumed that the supporting structure was made entirely of S235 steel, which is commonly used in building construction. The steel behaviour is described by a linear elasto-plastic law with strain hardening that involves four parameters: the Young modulus E_y, the yield strength f_y, the ultimate strength f_u and strain ε_u. Their numerical values used in the FE simulations are provided in Table **??**. In the absence of tests carried out on steel elements after the collapse, mean values of steel strengths were used in the FE model based on the new Eurocode for design of steel structures: f_y = 1.25 x 235 = 294 MPa and f_u = 1.2 x 360 = 432 MPa, along with an ultimate strain ε_u = 20 % .

Material characteristics considered in the FE model for describing the behaviour of the entire structure. Parameter Notation Unit Value Type S235 – – Density ρ_s kg.m^{-3} 7850 Young modulus E_y MPa 210000 Poisson ratio ν – 0.3 Yield strength f_y MPa 294 Ultimate strength f_u MPa 432 Ultimate strain ε_u - 0.2

Two pressure fields corresponding to the dead weight of the sheet covering the lattice structure and the snow-induced loading are taken into account. They are reflected in the model by line forces applied over the total upper T-profiles of the roof. Values of these line forces, identified in Table **??** and **??**, depend on whether the T-profile is located on the perimeter of the lattice or inside and on the choice retained for the distribution of the snow pressure field. The uniform pressure due to the dead weight of the sheet is taken equal to 60 N.m^{-2}. The distribution of snow load can vary over time based on the deflection observed on the lattice roof and its interaction with the dynamics of the snow cover. We believe that the distribution of the initial snow load (before rainfall) was nearly uniform due to the low slope of the roof and the light wind during snowfall. Then, rain likely first accumulated on the west and east edges of the roof until the direction of the slope of the roof changed due to an increase in deflection (i.e. when the deflection of the roof became too important and counter-balanced the initial 22.5 cm roof height).

All the rainwater is assumed to have remained on the roof until the building collapsed because the outlets were blocked by snow. After that, rainwater accumulated in the center of the roof. Therefore, three different cases of pressure distribution were studied, as shown in Figure 7: a uniform distribution, a case where water rapidly flowed on the edges of the roof, and a case where water mainly accumulated in the center of the roof. In the case of a uniform distribution, the pressure mimicking snow load varies between 0 and a maximum pressure of 4 905 $N.m^{-2}$ (Table **??**), which corresponds to a two-meter high snowpack with a density of 250 $kg.m^{-1}$ or a one-meter high wet snowpack with a mean density of 500 $kg.m^{-1}$. In the other two cases, snow-and-rain line loads applied to the structure after rainfall are identified in Table **??** based on the location of the T-Rebars mentioned in Figure **??**.

The dead weight of the structure is also taken into account, considering a steel density of 7 850 $kg.m^{-3}$ (see Table **??**).

Three different assumptions made for the distribution of snow and rain loads on the roof.

No wind loads were taken into account in this study, as wind effects were deemed negligible on the day the structure collapsed.

Since the roof frame elements are not hinged in the real structure, the roof frame has been modelled in one piece with rigid connections between elements. The links between the roof frame and the supporting tubular pylons are actually of a pivot type in the direction parallel to the facades to withstand the wind. Since the loads taken into account in the FE model are all vertical, this hinge is not supposed to be applied. A FE model with pivots has however been tested; both models led to similar results. A rigid linkage between these elements has therefore been taken into account in the model. To finish, all the columns of the facades are embedded.

Applied line loads to the structure during the pushover FE simulations in the case of a uniform distribution. Location of the T-profile Roof weight $N.ml^{-1}$Snow-and-rain weight $N.ml^{-1}$Roof perimeter 45 0 to 3679 Inside the roof 90 0 to 7358

Snow-and-rain line loads $N.ml^{-1}$applied to the structure during the pushover FE simulations in the case of pressure distribution with accumulation on the sides and central accumulation. T-profile rebars location NS WE ext WE int NS WE ext WE intA 6867 6867 13734 490.5 490.5 981B 12753 5886 11772 1962 1471.5 2943C 10791 4905 9810 3924 2452.5 4905D 8829 3924 7848 5886 3433.5 6867E 6867 2943 5886 7848 4414.5 8829F 4905 1962 3924 9810 5395.5 10791G 2943 981 1962 11772 6376.5 12753H 1226.25 245.25 490.5 13488.75 7112.25 14224.5

Location of the T-rebars affected by snow-and-rain loading.

3.2 FE simulations' results

It is important to stress here that one difficulty may arise from the fact that the initial The initial state of the building before the event is known with some uncertainty. In particular, past damage may have already occurred before the event of 2018 event and altered the initial integrity of the structure.

In fact, even though the studied building For example, although the building studied is not located in an area with intense snow events, it has had to support heavy loads on (at least) three times in the past occasions since its construction:

- around 27 27 cm on January 14-16, 1987;

- around ~~28~~ 28 cm on January 22, 1992;
- less than ~~10~~ 10 cm on March 7, 2010.

~~To~~ It is important to note that the snow event of January 22, 1992 was probably followed by rain, for which SAFRAN records provide a cumulative amount of 8 mm of rain approximately 36 hours after the snowfall. To the best of our knowledge, no survey ~~has been conducted on~~ of the structure of the Cévennes and Minéa buildings was carried out between the date of their construction and the 2018 incident. Following this event, only a technical opinion ~~of~~ on the strength of the adjacent Minéa building was requested. This report concluded that the overall strength of the structure was satisfactory, but identified a number of points requiring vigilance~~were identified~~:

- significant stagnation of ~~stormwater~~ rainwater on the roof;
- slight buckling (within manufacturing tolerance) and traces of corrosion on some profiles (angles and tubular profiles) at the level of the roof metal frame;
- buckling ~~on~~ of one of the profiles of a ~~Saint-André~~Saint-Andrew's cross;
- V-columns in satisfactory condition, with slight corrosion ~~at~~ on the head and anchor plate;
- ~~cracks and chips with visible reinforcement in concrete blocks used~~ presence of cracks (on several blocks) and spalling revealing the reinforcement (on one block) on the basal concrete blocks for anchoring the V-columns.

Given the limited information available on previous events and any damage that may have resulted from temporary loads applied to the structure in the past, this study has not taken into account any such deterioration of the structure.

~~However, it is worth noting that no modifications~~ Finally, it should be noted that no changes were made to the supporting structure from the time of its construction to the time of its collapse. The only changes made were ~~interior fittings (mezzanines supported by the ground~~to the interior (ground-supported mezzanines) in 2014.

~~Firstly, quasi-static pushover tests carried out by varying the pressure due to snow load. They can lead to the failure of the supporting structure, considering the different following criteria.~~

3.2 Distribution of the snow-and-rain loads on the roof

~~The first two failure criteria considered correspond to the attainment of two stresses states: (i) an accumulation of stresses equal to the yield strength of steel in a certain part of the model, which causes the elastic model to diverge (yield limit)~~ We have little information about the depth and spatial distribution of the initial snow on the roof. As the entire site was evacuated in the early afternoon of March 1, only the caretaker was present at the time of the building collapse, but he did not observe how the snow was distributed on the roof. Given that the wind velocity on both days was only between 1 and ~~(ii)an accumulation of stresses equal to~~ 4 $m.s^{-1}$, it is unlikely that the wind could have affected the distribution of snow on the roof. However, the distribution of the snow-and-rain load may have varied over time due to a complex interaction between the overall structure

and the dynamics of the snow cover, which gradually became wet. It seems likely that the distribution of the initial snow load (before rainfall) was nearly uniform due to the low slope of the ~~ultimate strength of steel, causing the elasto-plasic model to diverge (ultimate limit) . These criteria indicate the onset of deterioration that could potentially have a significant impact on the structure .~~ roof combined with the light wind during the snowfall. As indicated in Section 2.4, it is assumed that the rainwater remained on the roof until the complete collapse of the building. In order to try to gain some insight into different scenarios of spatial load distribution, three different (virtual) cases are studied, as shown in Figure 7a:

(a) **Uniform distribution**: reference case where the load distribution due to snow and rain is uniformly distributed,

(b) **Non-uniform with greater water depth at the edges**: water flowed rapidly towards the edges of the roof (assuming that the slope angle was sufficient),

(c) **Non-uniform with greater water depth in the center**: water mainly accumulated in the center of the roof.

For the two non-uniform distributions, we considered a snow load distribution that was initially uniform before rain came into play, as in the first case.

~~Two other failure criteria are based on the next two beam deflections: (iii)~~

3.3 FE simulations

In order to investigate in detail the mechanical response of the Irstea Cévennes building and thus better understand its collapse under the snow-and-rain load, the ~~vertical displacement equal to $l/200 = 0.225$ m and (iv) the vertical displacement equal to $L/200 = 0.27$ m and another one is (v) the maximum horizontal displacement at the top of the columns equal to $H/150 = 0.047$ m~~metal supporting structure was modeled using different Abaqus Finite Element (FE) models (see Section S2 in the SM for additional details). Two types of analysis are performed:

1. The **pushover analysis** provide load values associated with different types of failure criteria which can be interpreted as critical impacts on the structure with different levels of severity,

2. The **buckling analysis** indicate what specific elements of the structure were the most likely to be at the origin of the roof collapse.

Pushover analyses are quasi-static analyses (without dynamic effects) that determine how far the building can go before it collapses completely or partially. Figure 7 illustrates the main steps of this analysis. The first step (Step 1 in Figs. 7b-c) takes into account the self-weight of the structure. Then the snow-and-rain pressure on the structure is gradually and linearly incremented to mimic the load increase during the rain-on-snow event until the structure fails by reaching either the elastic limit of the material or the ultimate limit of the material for a snow-and-rain pressure equal to the failure force. This linear increase is performed in one step for uniform loads (step 2 in Fig. 7b) and two steps for non-uniform loads (steps 2 and 3 in Fig. 7c). In the latter case, step 2 corresponds to the increase of the uniform load of snow before the rain whereas step 3 corresponds to the increase of the non-uniform load of water on the snowpack.

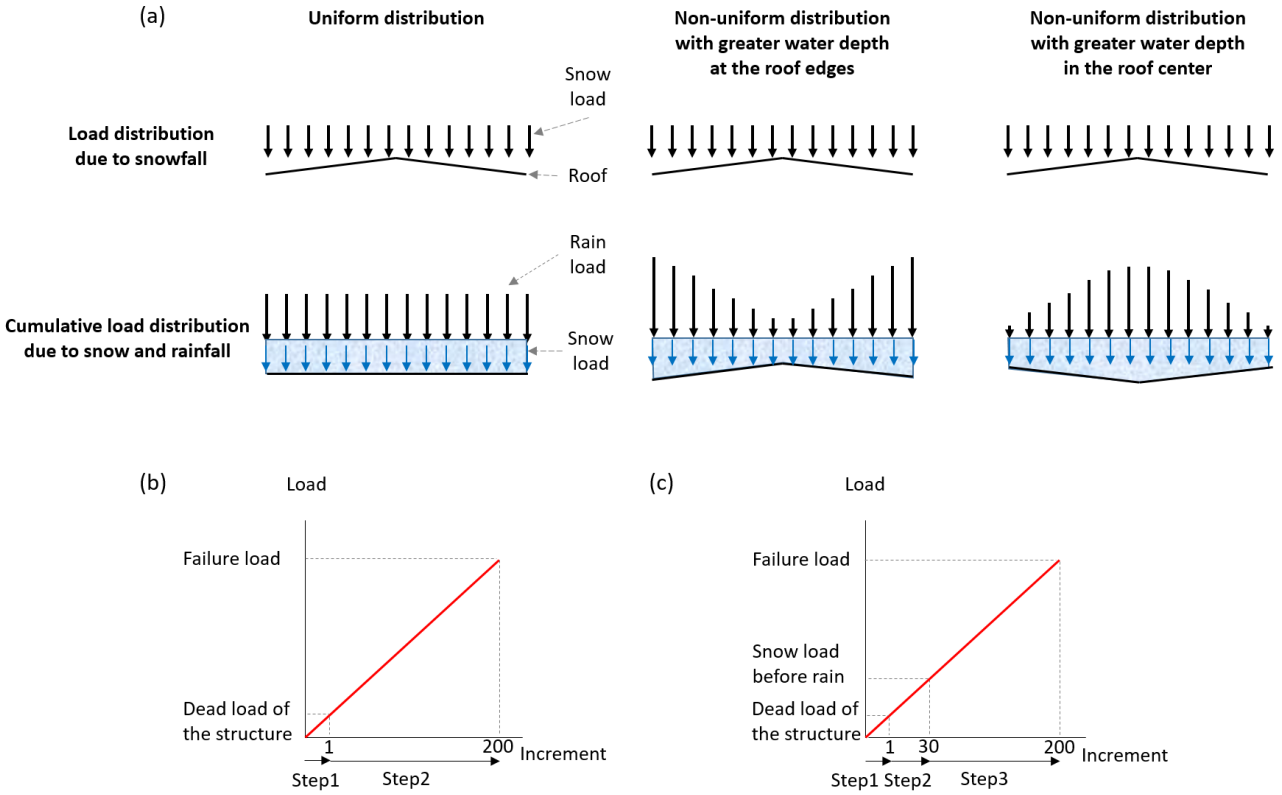

Figure 7. (a) Different assumptions made for the spatial distribution of snow-and-rain loads and (b), (c) load evolution by incrementation for pushover analyses in the cases of a uniform distribution (b) and a non-uniform distribution (c) of rain loads. Note that the increment numbers of steps 2 and 3 are given here as examples only.

Secondly, a non-linear buckling analysis ~~was performed~~ is carried out in two steps:

~~- a linear buckling analysis was conducted~~

1. A linear or eigenvalue buckling analysis is performed to obtain the ~~first fourteen buckling mode shapes~~ theoretical load values at which buckling of the structure~~and their corresponding eigenvalue buckling loads~~, idealized as elastic, occurs with different buckling mode shapes (so-called eigenvalue modes), as shown in Figure 8. This analysis ~~was~~ is carried out by ~~applying a vertical snow pressure of 1 Pa~~using the subspace iteration method (a simple method for approximating the eigenvalues of matrices), after a static step that ~~accounted for the dead load~~ takes into account the self-weight of the structure;

~~- a~~

2. A non-linear buckling analysis ~~(using the~~ is performed by using the incremental static Riks procedure ~~) of the FE model was conducted, integrating~~ of Abaqus, integrating material non-linearities and geometric imperfections corresponding

to the displacement results of the ~~pre-buckling~~ linear buckling analysis, in order to estimate the ~~critical bifurcation snow~~ most realistic critical buckling bifurcation pressure. Only the first mode shape ~~was taken into account, and the corresponding displacements were~~ is considered to define the geometric imperfections. The corresponding displacements are multiplied by an argument equal to ~~1 % of the crossbars thickness~~ 1 % of the thickness of the crossbar, *i.e.* ~~0.5~~ 0.5 mm, which corresponds to the manufacturing tolerance ~~value~~ of a round tubular profile with an ~~outside~~ external diameter of less than ~~75 mm.~~ 75 mm.

~~This analysis allowed to obtain (vi)~~These numerical tests do not describe the full (dynamic) collapse of the roof, but are intended to identify the critical loads at which significant deformation and damage could start to occur before the collapse, considering different failure criteria (FC):

- FC_{BD}: deflection threshold equal to 0.225 m, which corresponds to the acceptable beam deflection (vertical displacement that can be observed at the center of the roof) equal to 1/200 of the width of the building $l = 45$ m;
- FC_{HD}: horizontal displacement threshold at the top of the columns equal to $H/150 = 0.047$ m;
- FC_y: critical stress state with an accumulation of stresses equal to the yield strength of steel in a given location of the FE model. This so-called *elastic limit* indicates the limit of the elastic behavior of the structure, i.e. the beginning of irreversible deformations;
- FC_u: critical stress state with an accumulation of stresses equal to the ultimate strength of steel. This so-called *ultimate limit* of the material corresponds to the maximum load that the structure can withstand before a local material rupture;
- FC_{LB}: first eigenvalue buckling load assessed by the linear buckling analysis;
- FC_{NLB}: non-linear buckling load corresponding to the ~~first linear buckling load and (vii) the~~ bifurcation buckling load that causes the actual buckling, taking into account the geometric imperfections.

The first two failure criteria deal with global damage to the structure and are part of the Serviceability Limit States (SLS). The other failure criteria correspond to Ultimate Limit States (ULS). These criteria indicate the onset of deterioration that could potentially have a significant impact on the structure and ultimately lead to its collapse.

Table 1 ~~presents the (~~summarizes the different critical load values obtained from the FE simulations that lead to the failure of the structure, considering the different criteria mentioned above, under the three different assumptions of snow-and-rain ~~) load values that result in structural failure according to the different failure criteria for the three assumptions of snow loads distributionon the roof. They typically range between~~ load distribution. The values obtained for these critical loads vary over a wide range from 645 ~~and~~ to 3 410 $\mathrm{N.m^{-2}}$ depending on the ~~selected~~ failure criterion and the ~~assumption of pressure field distribution. The beam deflection and elastic criteria provide intermediate failure pressure values between the lowest and the highest values obtained from the buckling criterion and the ultimate limit or horizontal displacement criterion, respectively. However, for non-uniform snow pressure fields, the ultimate limit is not reached due to code divergence.~~

The snow loads that cause buckling, as obtained from the FE simulations, are similar regardless of the distribution of the snowpack. This is because the load that causes buckling (645 kN.m^{-2}) is lower than the pressure exerted by a uniform snowpack of 30 cm thickness (which is 735 kN distribution of the pressure field. Section 4 further discusses these different critical loads and compares them with the estimated snow-and-rain load of about 1 226 to 1 325 N.m^{-2}). However, when considering other criteria, the case of a central accumulation of snow always proves to be the most critical. provided in Section 2.

Table 1. Snow load Load values leading to the failure of the supporting structure for calculated from the FE simulations according to different failure criteria (see text for details), and considering three scenarios for the distribution of the snow-and-rain load: uniform distribution (snow and rain), non-uniform distribution with greater water depth at the edges after uniform snowfall, and non-uniform distribution with greater water depth in the center after uniform snowfall. The last line of the table indicates the loads at which code divergence was observed (when the considered failure criterion was not reached).

Note that we restrict here our discussion to snow loads expressed in pressures, as pressure is the input parameter in the FE modelling. How those pressu

7 1 099.6 1.318 East facade8 1 105.2 1.353 East facade9 1 271.2 1.385 West fac

First buckling mode shape of the structure, located over the west facade. The FE simulations allow us to gain further insight into the detailed behavior of the structure. Figure 9 shows the stress fields of the structure obtained from the pushover simulations and corresponding to the three types of distribution for a snow-and-rain load of 1 325 N.m^{-2}. In the three cases, the maximum stresses occur on the crossbars located at the perimeter of the roof (above the western and eastern facades in the two first cases and above the four facades in the last case) and, in the cases of uniform distribution and non-uniform distribution with greater water depth in the center, on the bottom horizontal T-profiles located in the central part of the roof. Stresses (slightly) above the yield strength of the material occur only on two crossbars located above the east facades and are prone to buckling.

The results of the linear buckling analysis for a uniform snow-and-rain pressure field are summarized in Table 2 and Figure 8. According to the analysis , 2 and in Figure 8. The analysis shows that buckling occurs locally. For each of the fourteen eight first eigenvalue modes , only two crossbars located on the considered, only one or two crossbar(s) located at the western or eastern

Table 2. Results of the eigenvalue buckling analysis of the structure (linear buckling) under a uniform snow-and-rain pressure field.

Eigenvalue mode	Corresponding load [N.m^{-2}]	Corresponding displacement [m]	Location of the buckling crossbars
1	934.6	1.373	Western facade
2	937	1.366	Western facade
3	939	1.279	Western facade
4	941.1	1.277	Western facade
5	1051.3	1.241	Eastern facade
6	1055.5	1.392	Eastern facade
7	1099.6	1.318	Eastern facade
8	1105.2	1.353	Eastern facade

perimeter of the roof and on either side of the east-west axis of the structure buckle with a shape similar to ~~the one~~ that of the first ~~mode~~ and fifth modes shown in Figure 8. Table 2 provides information ~~about the buckling loads, displacements, and the~~ on the buckling load, displacement, and location of crossbars prone to buckling for each eigenvalue mode. ~~The table~~ It shows that buckling occurs first at the crossbars above the ~~west~~ western facade and then above the ~~east~~ eastern facade. Similar results (not shown) are obtained for the other ~~cases of~~ two cases of non-uniform snow-and-rain pressure ~~distributions.~~ distribution with greater water depth either at the edges or in the center of the roof.

~~Figure 9 depicts the stress field of the structure at the last convergence step obtained by the pushover simulations in the cases of a pressure field with an accumulation on the sides and a central accumulation. In both cases, the maximum stresses occur at the bottom horizontal T-profiles located in the central part of the roof and at the crossbars located on the perimeter of the roof. In the case of a pressure field with accumulation on the sides, more crossbarson the perimeter of the roof, particularly above the west facade, yield and buckle, while more horizontal bars in the center of the roof yield in the case of a pressure field with a central accumulation.~~ These results clearly indicate that ~~failure occurred~~ the failure was due to both buckling of the crossbars (primary cause) and bending of the bottom horizontal T-profiles (aggravating effect). Other damage, such as ~~those~~ that observed on the round tubular ~~poles as~~ columns shown in Figure ~~**??c and ??d, likely occurred after,**~~ S3c-d in the SM, probably occurred during the collapse of the structure. No such damage was observed on the nearby building, whereas slight buckling ~~phenomena were identified~~ was observed on its roof. This subsequent damage was further modified by the presence of the offices and mezzanine walls along the ~~north and south facades as shown in Figure **??**e~~northern and southern facades (see Fig. S3e in the SM).

~~(a)(b)Von Mises stress field inside the structure at the last convergence step, given by the FE model simulation for a snow pressure field with (a) an accumulation on the sides and (b) a central accumulation.~~

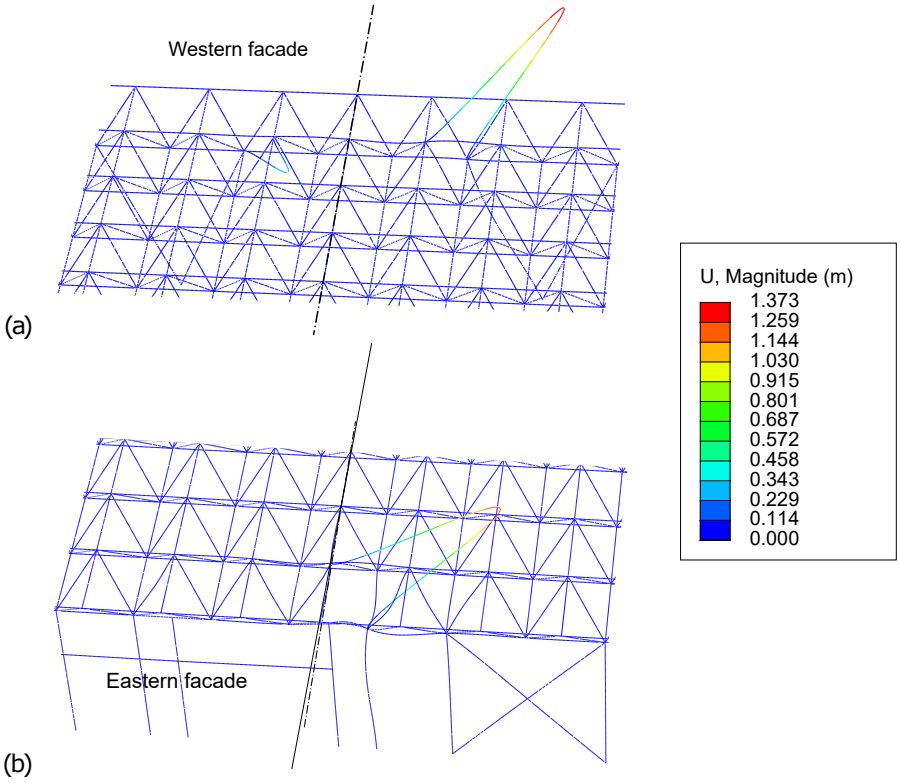

Figure 8. Buckling mode shapes of the structure under a uniform snow-and-rain pressure field (deformation scale factor = 5.4): (a) first mode, above the western facade and (b) fifth mode, above the eastern facade.

4 Discussion

This ~~discussion section intends to make the link between~~ section aims to further link the results from the ~~snow and rain~~ snow-and-rain hazard (Section 2) and from the ~~quasi-static pushover FE simulations~~ FE simulations that include pushover tests and a buckling anlysis (Section 3) ~~, in order to provide~~ to identify the most probable ~~scenario which~~ factors that led to the collapse of the Irstea Cévennes building.

4.1 Building collapse analysis under the rain-on-snow event of February 2018

Figure ~~10 graphically summarizes the results of the quasi-static pushover and buckling FE simulations in the case of a uniform pressure distribution. Based on the hydrostatic pressure assumption ($\rho g h$), the iso-pressure curves corresponding to the different failure criteria used (see~~ 10 compares the critical loads that would cause a failure according to the FE simulations

(Table 1) ~~can be plotted in the $(\rho, h)-$plane and this defines the safe and unsafe zones for the structure in terms of snowpack height h and density ρ.Below the dashed red-colored line (buckling limit), the structure remains intact. Above the continuous red-colored line (ultimate criterion), the structure collapses.In between (hatched zone in Figure 10) , the structure undergoes irreversible damage that is more and more significant when approaching the continuous red-colored line. The dashed-dotted, dotted, and fine dashed-dotted red-colored lines define the yield limit , curvature limit based on the deflection of the structure, and horizontal displacement limit, respectively. Additionally, the buckling load obtained via the linear buckling analysis is represented by the fine dashed red-colored line.~~

~~The analysis of the chronicle of the climatic event described in Section 2 led to an initial snow depth on the ground (before rain)that certainly ranged from 30~~ with the initial snow load of 736 N.m^{-2} before the rain and the final snow-and-rain load values of 1 226 to ~~35 cm and an initial snow density likely to be around 250 kg.m^{-3}. In this study, the snow load on the roof has been estimated to be equal to the snow load on the ground due to several reasons. Firstly, the roof slope was low, and a small wall was present around the edges of the roof.Secondly, the wind was not significant enough (force 1) to modify (reduce) the snow height on the roof. Lastly, no shape factor was used to estimate the snow load on the roof.~~ 1 325 N.m^{-2} estimated from different source of observations in Section 2.

~~The corresponding two pairs of values (density ρ and height h, before rain~~The maximum critical load of 3 410 N.m^{-2} (in red in Figure 10) ~~can be displayed in~~ corresponds to the ultimate limit of the ~~$(\rho, h)-$plane of Figure 10, as depicted by the blue-colored triangles and circles. These two points can be directly compared to the iso-pressure curves inferred by the FE Abaqus simulations: they remain below the limits related to linear buckling , curvature, horizontal displacement, and material properties but are above the~~ material under uniform pressure distribution and is well above the estimated value for the snow-and-rain load of 1 226 – 1 325 N.m^{-2} (in cyan). Note that for non-uniform snow pressure fields, the ultimate material limit is not reached due to numerical instabilities (lack of convergence). The values obtained from the horizontal displacement criterion are also quite above the estimated range of 1 226 – 1 325 N.m^{-2}. The pushover FE simulations thus suggest that neither the ultimate material limit nor the critical horizontal displacement was reached at the time just before of the collapse, regardless of the scenario for rain load spatial distribution.

The minimum of 645 N.m^{-2} (in brown) corresponds to the non-linear ~~buckling limit that takes into account initial geometric imperfections (estimated to be 645~~ buckling load. This value is just below the uniform initial snow load before the rain (736 N.m^{-2}) (in teal) and does not depend on the assumption made for the distribution of the rain load. In contrast, the linear buckling analysis gives higher values for the load corresponding to the first eigenvalue mode (from 935 to 945 N.m~~$^{-2}$; see Table 4). They remain~~ $^{-2}$). All of these critical buckling loads (in beige) are well below the ~~load leading to the full collapse of the building, which is estimated to be 3 410 N. m^{-2}, as given by the ultimate limit criterion (see Table 1. Therefore, it can be safely concluded here that the initial snowfall (before rain)was critical for potential irreversible damage (buckling) to the structure, but it is unlikely to have been the sole cause of the full~~ snow-and-rain load estimates. This means that this failure can have occurred with the observed snow-and-rain load. In addition, although it should be noted that the buckling failures remained localized (on a few crossbars located at the eastern and western edges, as shown in Section 3 and Figure 8), they

occur on both sides of the east-west axis along which the structure collapsed, as shown in Figure 6d. Thus, it is very likely that buckling was involved at some stage in the roof collapse.

As analysed in Section 2, the snowfall was followed by rain: during that rainfall, we consider that the snow cover density may have increased up to around 600 kg.m^{-3} due to partial saturation of the snowpack with water available. In reality, the wet snowpack was likely heterogeneous with areas of soared snow at higher densities (300-400 kg/m3) than the initial snow (250 kg/m3) and other areas at the bottom with accumulated water (1 000 kg/m3) due to preferential water flows. The value of 600 kg/m3 corresponds to an equivalent value used to define the (equivalent) pressure exerted by the combination of snow and rain accumulations. Predicting the evolution of the snowpack after rain and its interaction with the deforming structure is difficult and we may expect some complicated dynamics that potentially produced a non-uniform pressure field during the rain event. In want of any monitoring or any full modeling of the snowpack evolution over time during the rain-on-snow event of 2018 and its interaction with the structure, we consider here one (simplified) scenario with no settling ($h = cste$) but a gradual increase of density due to water. This scenario is represented by the blue-colored horizontal lines drawn in Figure 10. Depending on the initial snow height and the ultimate limit reached for the density of the very wet snowpack after rain, this defines (ultimate) points that remain in the intermediate hatched zone for which the structure undergoes irreversible deformation. These points are still above safe limits in terms of buckling, yield, and deflection. As such, it can be concluded that the rain added to the snow cover initially in place certainly led to severe irreversible damage to the structure. For a uniform load distribution, the other failure criteria (the elastic limit and the beam deflection) give intermediate values in the range $1\,330 - 1\,360$ N.m^{-2}, just above the snow-and-rain load estimates. For the scenario with greater water depth at the edges, the critical load values increase, particularly for the beam deflection criterion, which puts the structure on the safe side. For the scenario with water flowing towards the center of the roof, both critical load values (elastic limit, beam deflection) decrease close to or below the snow-and-rain load estimates.

There are several sources of explanation for the fact that our analysis displayed on Figure 10 does predict irreversible damage but not a full collapse of the building. One reason is associated with the initial state of the structure which we assume as perfect with no previous damage experienced by the structure. An unknown initial damage which would have been In summary, the FE simulations indicate different situations where the critical load values were below (or very close to) the snow-and-rain load estimates and thus could lead to critical damage and failure of the structure during the 2018 snow-and-rain event. According to the linear and non-linear buckling analysis, buckling has likely been critical regardless of the scenario for the distribution of the snow-and-rain load, indicating a weakness in the structure. In addition, based on the elastic limit criterion and the beam deflection criterion, load concentration in the center of the roof (most likely due to water accumulation in the center of the roof) has probably been at some stage an aggravating factor. However, it must be pointed out that the order and the interactions between these different mechanical responses (buckling, beam deflection) are not taken into account in the FE simulatons could have easily brought the horizontal blue lines in the red zone. Another reason is that pushover simulationsdo not account for the buckling of the structure, while post-buckling analysis fails to predict the collapse of the structureby the FE simulations.

4.2 Structural back analysis

In ~~Appendix ??~~Section S3 of the SM, we discuss in detail the regulations ~~: the one in place~~ on snow action on structures: those in force at the time of the construction of the Irstea Cevennes building and those in force at the time of the ~~one when the~~ building collapse~~under snow load occurred~~. By comparing the regulations ~~to the FE Abaqus~~ with the FE-Abaqus calculations in terms of the ~~applied stresses~~ load applied to the structure~~(see Figure ?? and related text in Appendix ??)~~, we show that the Irstea Cevennes building was ~~correctly built in accordance with~~ certainly built correctly according to the previous French regulations (~~dating back to~~ of 1965), ~~without accounting for any steel imperfections . We also conclude thatthe building~~if we do not take into account the results of the non-linear buckling analysis, since the consideration of imperfections in the design of metal structures was introduced in the regulations after the construction of this building (in 1983). It can also be concluded that, at the ~~moment~~ time of its collapse in 2018, ~~was not respecting~~ the building did not comply with the new regulations; ~~indeed~~in fact, the critical buckling load of the structure (estimated at 645~~N.~~ N. m^{-2}) ~~, and the lower estimate of the load required to cause a deflection of 0.225 m (equal to 1 205 $\mathrm{N.m}^{-2}$) were lower than the exceptional snow load specified in~~ was lower than the design accidental snow load resulting from the Eurocode (equal to ~~0.8 x 1 350 + 200 = 1 280~~ 1 280 $\mathrm{N.m}^{-2}$, see Section S3 in the SM).

~~In this subsection , attention is paid to~~ This subsection aims to identify the weaknesses of the structure subjected to the ~~identification of specific structural weaknesses which may have been critical, in so far as the FE simulations showed that structural weaknesses, combined with the~~ extreme climatic event ~~, can further~~ (the estimated snow-and-rain load of $1\,226 - 1\,325$ $\mathrm{N.m}^{-2}$ was indeed close to the design exceptional snow load specified in the Eurocode, see Figure S8 of the SM) to possibly explain the collapse.

Firstly, as indicated above, ~~crossbars located at the~~ the crossbars at the eastern and western perimeter of the lattice roof ~~are~~ were clearly prone to buckling. Although this buckling ~~is~~ was localized, it gradually ~~weakens~~ weakened the structure and could ~~potentially lead~~ have potentially contributed to its collapse. Similar phenomena were also observed in the nearby building after the 2018 incident ~~on the nearby building.~~

~~Secondly, insofar as large-size~~ (Fig. 6). Secondly, since large vehicles (agricultural tractors) were to be used inside the building, no load-bearing walls were built inside. This ~~led to the design of~~ resulted in a very large span of the roof supporting lattice. ~~Thus, our FE simulations suggest that the excessive~~ Even if the deflection threshold FC_{BD} is respected, the FE simulations show that the snow-and-rain has led to an important deflection of the lattice ~~is one cause of the collapse of the building under the rain-on-snow event of 2018.~~ (Fig. 9). It should be noted that ~~a neighbour building(see Figure 6)~~the nearby building, similar to the one ~~which~~ that collapsed, resisted the ~~event of~~ February 2018 event and is still ~~in place~~ standing on the site. This ~~neighbour structure houses~~ nearby building contains a number of offices and therefore ~~includes some inner~~ has some internal load-bearing walls. This may be an ~~evidence that the latter walls inside the structure may be efficient to prevent significant deflections. This feedback could be considered in the future to encourage greater attention to the design of long-range roofs, particularly in the context of climate change leading which increases the uncertainties about the frequency and intensity of future rain-on-snow events~~indication that these latter walls within the structure are likely to be effective in preventing significant deflection.

Finally, the roof rain drainage system, consisting exclusively of vertical openings ~~positioned~~ located in the lower part of the roof perimeter (see Figure ~~??) , did not allow for the evacuation of rain once the roof was covered with snow . Indeed, significant water stagnation was observed on the roof of the similar nearby building a few days after the 2018 incident. Such a device thus led~~ S5 in the SM) combined with a near-flat roof, probably contributed to a very poor evacuation of the rain immediately after the snow event, leading to a significant increase ~~of the load supported by the lattice. This is another strongest structural weakness of the building, as evidenced by the following two scenarios considering no water evacuation, as depicted on the plots of Figure 10 (horizontal blue lines).~~ in the load carried by the roof. In the future, it would be interesting to ~~conduct~~ perform more thorough studies of rainwater drainage on near-flat roofs during rain-on-snow events, following the efforts made by Colbeck (1977); O'Rourke and Downey (2001); Otsuki et al. (2017). It is important to clarify the effectiveness of ~~various~~ different drainage solutions under snowy roof conditions, and to ~~provide corresponding~~ make appropriate recommendations regarding the required roof slopes and the selection and design of downstream ~~evacuation~~ drainage devices.

4.3 ~~Characteristic snow loads in this region in a context of climate change~~

~~The rarity of large snow events at low elevations in this Mediterranean region makes the estimation of characteristic snow loads complex. Winters are generally mild in this area, with a low percentage of days below 0°C along the coasts. Significant snow events occur only every few years, and the high presence of zeros in the series makes the statistical treatment more difficult, as it is the case for low-latitude high-elevation zones (O'Donnell et al., 2020).~~

~~In a context of climate change, the French Mediterranean region, like most regions of the planet, is warming significantly (IPCC, 2021) . Many studies have shown that extreme precipitation (snow and rain) events also intensify in this region in past observations (Ribes et al., 20 and according to climate projections (Tramblay and Somot, 2018). Concerning snow load extremes, future trends in this non-mountainous region are unclear, for several reasons:~~

- ~~While extreme daily precipitation intensities are increasing, snow events become rarer as a result of global warming (snow events becoming rain events). It is not clear if extreme daily snow accumulations are decreasing if the occurrence of below-zero temperatures remains important.~~
- ~~Climate models do not provide snow variables. While some studies provide projections of future snow conditions (e.g. Verfaillie et al. , they are usually restricted to mountainous regions.~~
- ~~Reports on the cryosphere generally focus on mountainous areas or high latitude areas (IPCC, 2019).~~

~~As a consequence, very few studies provide insights about past and future trends of snow loads in the region around Montpellier city. However, Croce and Landi (2021) recently show that characteristic snow loads are projected to increase along the coastlines of the French Mediterranean region. These results have important implications for current French standards, which have been established assuming 1/ a stationary climate (i.e. ignoring climate changes) 2/ a regional homogeneity, French standards being provided over large areas.~~

5 Conclusions

Using multiple sources of information regarding the 2018 meteorological event in terms of snow and rain amounts and detailed simulations of the ~~behaviour~~ behavior of the roof structure subject to loads, this study provides a detailed back analysis of the interactions between the snow cover and the structure. Concerning the meteorological event, while intense snow events are unusual in this area, this type of event ~~is not exceptional and occurs~~ can occur when winter storms bring important masses of cold air from northern Europe to the south (see the recent event in Madrid Smart, 2021). In Montpellier, snow depths around or above 30 cm have been recorded several times in the past (~~35~~ 35 cm in February 1954, ~~35~~ 35 cm during winter 1962-1963, ~~27~~ 27 cm on the ~~14-16/01/~~14-16th of January 1987, ~~28~~ 28 cm on the ~~22/01/~~22nd of January 1992). For this event in Montpellier, the snow-rain transition led to a saturated and ~~overweighted snowpack~~overweight load. A detailed understanding of the meteorological event has been consolidated using various sources of information: weather stations, numerical weather model outputs, meteorological reanalysis, and numerous testimonies obtained using social networks (~~facebook~~Facebook).

This study proposes an assessment of the response of the structure to ~~the load~~ incremented load values under quasi-static conditions, as well as a buckling analysis. Different scenarios for ~~distributions~~ the distribution of the pressure field imparted to the structure have been studied~~, as both the behaviour of the snow cover during the rain-on-snow event and the response of the structure are transient and non-uniform processes, for which the properties evolve gradually over time and space~~. Based on the results obtained, the collapse of the Irstea Cévennes building can be explained by ~~two main factors. Firstly~~a combination of several factors. First, the structure was ~~weak against buckling andbending, despite being~~ susceptible to significant buckling and, to a lesser extent, to bending (although it was designed in accordance with the regulations ~~at the time it was built~~on this aspect). Secondly, the collapse ~~may have been contributed to by the intensity of the~~ was probably caused by the rain-on-snow ~~event, as well as the fact that the rainwater was unable to flow due to the low slope of the roof and the small 20 cm drainage openings. These openings were likely blocked by the dense snowpack that had already accumulated when the precipitation turned into rain. Thus, it is~~ surcharge. Furthermore, it seems evident that geometric imperfections were not considered ~~during~~ in the design of the structure, resulting in its vulnerability to buckling ~~. Moreover, the snow cover started saturating and the~~ (also observed in the neighbouring Minea building). The fact that the resulting load exceeded the critical load leading to roof failure is certainly due to the additional water on the initial snowpack. Such a rain-on-snow scenario is considered in the regulations but it appears that in the particular chronicle of the 2018 event (significant amounts of snow and then ~~of water with varying temperature conditions)~~rain), the resulting overload was greater than the design scenario.

~~In conclusion, this study has shown that some older metallic buildings, whose design did not take into account imperfections, may be at risk of buckling during exceptional rain-on-snow events. Additionally, inadequate rainwater drainage can also enhance this risk. Therefore, it would be interesting to conduct research in the near future to determine the effectiveness of different rainwater drainage systems for relatively flat roofs where a high level of snow accumulation can occur during snow events followed by intense rainfall. This would facilitate the development of recommendations on the subject in the future.~~

~~The evolution of intense snow events, in a context of climate change, is particularly unclear because of concurrent factors. While precipitation extremes are expected to intensify in this region (Tramblay and Somot, 2018), we expect more precipitation~~

events falling as rain instead of snow in this region. However, climate models simulate important changes in the dynamics of these events, and very few studies (at the exception of Croce and Landi, 2021) assess extreme snow events in non-mountainous regions.

Author contributions

TF coordinated and supervised the back-analysis study. GE and DR performed the analysis of the meteorological event meteorological event analysis. IO carried out the FE model simulationsof the loaded building and proposed a first comparison between the FE simulations' results and the analysis of the snow and rain hazard. All authors discussed the results and co-wrote the manuscript.

Competing interests

The authors declare that they have no conflict of interest.

Acknowledgements

The authors thank Mohamed Naaim for having motivated this research. They are grateful to Meteo-Languedoc and Meteociel for sharing the meteorological information and resources. They also thank Jean-Luc Descrismes and Sylvain Labbé of INRAE for having provided all available information about the Irstea Cévennes building.

6 Additional information about the Irstea Cévennes building

This appendix gives some details about the Irstea Cévennes building, in addition to the information already provided in the main text (Section 3).

Figure ?? provides the location map of the Cévennes building in the Montpellier site of Irstea (now INRAE).

Location map of the Irstea Cévennes building in Montpellier. Source: Inrae.

Figure ?? gives close-up views of the different types of damage to the structure of the Irstea Cévennes building, as observed on March 18, 2018, a couple of weeks after the roof collapse.

Close-up views of damage to the structure of the Irstea Cévennes hall, as observed on March 18, 2018: buckling and bending failure of roof tubular profiles (a,b), bending and shear failures of tubular supporting pylons (c,d) and cracking of the inner offices' walls made of concrete and located along the southern face of the building.

Figure ?? gives a description of the geometry of the metal structure modelled by FE Abaqus software, including the details of the geometry of each component. The numerical values given to the different geometrical properties defined in Figure ?? are given in Table ??.

Details of the metal structure modelled by the FE Abaqus software: general view (a) and front view of one single roof frame element (b), round (c), and rectangular (d) tubular profiles' and HEA (e) and T- (f) profiles' features.

Geometrical properties of the structure Parameter Symbol Value Unit Global structure Roof wide l 45.00 m Roof length L 54.00 m Roof height h 1.90 m Total height H 9.90 m Top and (bottom) roof lattice T-profiles Wide b 160 (120) mm Height h_t 100 (80) mm Thickness t_f 9 (7) mm Thickness t_w 18 (14) mm Position of the local cross-section axis l_t 68.9 (54.5) mm HEA 160 Wide $b_1 = b_2$ 160 mm Height h 152 mm Thickness $t_1 = t_2$ 9 mm Thickness t_w 6 mm Round tubular profiles of roof lattice Outer radius r 24.15 mm Thickness t 2.9 mm Round tubular profiles of facades Outer radius r 109.55 mm Thickness t 4.5 mm Rectangular tubular profiles Height a 100 mm Wide b 50 mm Thickness t 2 mm

6 Analysis of the building collapse considering the regulations

The existing regulation for engineering snow load design in France at the time of the Irstea building construction in 1982 was the French standard which defines the snow and wind effects on construction, initially published in 1965 (CGNG, 2000). This French standard was based on geographical areas (regions I, II, III and a region III + 45%) for which snow loads on floor below 200 m above sea level were defined *a priori*. Table **??** gives the values of ground snow loads which had to be taken into account to design buildings located in the region II including Montpellier city.

Values of ground snow load N.m$^-$2to be considered according to the French NV65 standard published in 1965 for the region II where Montpellier city is located. Region II Normal overload 450 Extreme overload 750

Today, in compliance with Eurocode 1 and the NF EN 1991-1-3 standard adopted in France according to Eurocode 1 (CEN/TC250, 1991; AFNOR, 2004, 2007), snow load on a roof, s, is defined by the following equation:

$$s = \mu_i \cdot C_e \cdot C_t \cdot s_o,$$

where $s_o = s_k$ or s_{Ad}, and where s_k Finally, the authors are grateful to the Editor, Yves Bühler, and s_{Ad} are the ground snow loads for permanent/transitional and accidental project situations, respectively (with respect to the geographical zone under consideration). μ_i represents the roof shape coefficient that accounts for undrifted and drifted snow load arrangements, respectively, depending on the shape and the slope of the roof. C_e is the exposure coefficient (equal to 0.8 for a windswept site, 1 for a normal site and 1.25 for a sheltered site). C_t is the thermal coefficient (equal to 1 for a roof that has no high thermal transmittance).

Ground snow load values to be used in France are given for eight different zones depending on the altitude (those concerned by the present case are referred in Table **??**). They are determined on the basis of a probability that they will be exceeded over a one-year period (excluding the case of exceptional snow) equal to 0.02 and assuming a snow density of 150 kg.m^{-3}. Note that such a value for density corresponds to relatively dry and fresh snow and remains well below the typical density of humid snow (around 250 kg.m^{-3}), as involved in the present case study which concerns a Mediterranean area (see Section 2).

Values of ground snow load N.m^{-2}for the region where Montpellier city is located according to the NF EN 1991-1-3 standard published in 1991. Region B2 Characteristic value of ground snow load (s_k) at an altitude of less than 200 m 550 Design value of exceptional ground snow load (s_{Ad}) 1 350

Eurocode 1 also provides that in areas where rain on snow may cause melting followed by frost, snow loads on roof must be increased, especially if snow and ice can block the roof drainage system. The NF EN 1991-1-3 standard stipulates that roof snow load must be increased by 0.2 kN.m^{-2} when the slope for water flow is lower than 3 %, in order to account for the snow density increase resulting from difficulties of water drainage in case of rain.

In our case, the roof of the building being made of one single slope that is less than 30°, only one load case is to be considered in permanent project situation and $\mu_i = \mu_1 = 0.8$ for both permanent and accidental project situations with typical and exceptional snow loads, respectively.

So, in Figure **??**, roof snow loads leading to the failure criteria of the Cévennes supporting structure according to the FE model simulations in the most critical case of pressure field with a central accumulation (in the range 645 — 1 915 N.m^{-2} for criteria other than the ultimate limit) are compared to values (without safety factors) recommended by the French DTU NV65 standard, valid at the moment of the building construction in 1982 (450 and 750 N.m^{-2} for normal and extreme design loads) and the NF EN 1991-1-3 standard, adopted in application of Eurocode 1 ($0.8 * 550 + 200 = 640$ and $0.8 * 1\,350 + 200 = 1\,280$ N.m^{-2} for characteristic and exceptional design loads, respectively).

Comparison for different combinations of snow depth and density between the snow loads leading to the different failure criteria of the Cévennes building, as calculated by the FE model, and the snow load values recommended by Eurocode 1 and the DTU NV65 without taking into account safety factors (both in terms of loads and the steel behaviour law) in the case of a snow pressure field with a central accumulation.

In France, the consideration of imperfections in the design of metallic structures was introduced in the regulations in 1983, with the publication of the first version of the Regulation on Metal Construction, so after the construction of the building studied here. If initial geometric imperfections are not taken into account (linear buckling limit), and even more if the dead load of the structure is neglected in the estimation of the critical buckling load (linear buckling limit without dead weight), the results show that the structure begins to be damaged by snow loads (equal to 940 and 1 235 kN.m^{-2}, respectively) largely above the normal and extreme loads recommended by the DTU NV65, which are 450 and 750 kN.m^{-2}. It seems, therefore, that the design of this building was executed in accordance with the state of the art at that time.

Under current regulations, taking into account initial geometric imperfections, buckling occurs first for a load of 645 N.m^{-2} which is of the same order of magnitude as the characteristic design load (that corresponds to a snow load equal to 640 N.m^{-2}) and well below the exceptional load (equal to 1 280 N.m^{-2}) recommended by Eurocode. Moreover, in the case of a central accumulation of snowpack, the building fails serviceability (excessive deflection) for a load of 1 205 N.m^{-2} just less than the exceptional load recommended by Eurocode. It is therefore clear that this structure was not consistent with the current design basis rules. In contrast, the building begins to yield and fails serviceability from a horizontal displacement point of view for snow loads (equal to 1 325 and 1 925 N.m^{-2} respectively) largely above the characteristic project situation and above this exceptional load tooto the numerous referees for their insightful comments on previous versions of the manuscript.

References

AFNOR: NF EN 1991-1-3 : Eurocode 1 : Actions sur les structures - Partie 1-3 : Actions générales - charges de neige, Association Francaise de Normalisation (AFNOR), 2004.

AFNOR: NF EN 1991-1-3/NA : Eurocode 1 : Actions sur les structures - Partie 1-3 : Actions générales - charges de neige. Annexe nationale à la NF EN 1991-1-3, Association Francaise de Normalisation (AFNOR), 2007.

Altunişik, A., Ateş, S., and Hüsem, M.: Lateral buckling failure of steel cantilever roof of a tribune due to snow loads, Engineering Failure Analysis, 72, 67–78, https://doi.org/10.1016/j.engfailanal.2016.12.010, 2017.

ASCE: Minimum Design Loads for Buildings and Other Structures - ASCE/SEI 7-10, Tech. rep., https://law.resource.org/pub/us/cfr/ibr/003/asce.7.2002.pdf, 2013.

Biegus, A. and Kowal, A.: Collapse of halls made from cold-formed steel sheets, Engineering Failure Analysis, 31, 189–194, https://doi.org/10.1016/j.engfailanal.2012.12.009, 2013.

Biegus, A. and Rykaluk, K.: Collapse of Katowice Fair Building, Engineering Failure Analysis, 16, 1643–1654, https://doi.org/10.1016/j.engfailanal.2008.11.008, 2009.

Bouttier, F. and Roulet, B.: Arome, the new high resolution model of Meteo-France, The European forecaster - Newsletter of the WGCEF (Printed by Meteo-France), 13, 27–30, 2008.

Brencich, A.: Collapse of an industrial steel shed: A case study for basic errors in computational structural engineering and control procedures, Engineering Failure Analysis, 17, 213–225, https://doi.org/10.1016/j.engfailanal.2009.06.015, 2010.

Caglayan, O. and Yuksel, E.: Experimental and finite element investigations on the collapse of a Mero space truss roof structure – A case study, Engineering Failure Analysis, 15, 458–470, https://doi.org/10.1016/j.engfailanal.2007.05.005, 2008.

Canadian Commission on Building and Fire Codes: National Building Code of Canada: 2010, Tech. rep., National Research Council of Canada, https://doi.org/10.4224/40001268, 2010.

CEN/TC250: Eurocode 1: Actions on structures - Part 1-3: General actions - Snow loads (EN 1991-1-3), Comité européen de Normalisation / Comité Technique CEN/TC 250 "Eurocodes structuraux", 1991.

CGNG: Règles NV 65, modifiées en décembre 1999, avril 2000 et février 2009 et annexes. DTU P 06-002 : Règles définissant les effets de la neige et du vent sur les constructions., Commission Générale de Normalisation du Bâtiment, 2000.

Colbeck, S. C.: Roof loads resulting from rain on snow: results of a physical model, Canadian Journal of Civil Engineering, 4, 482–490, https://doi.org/10.1139/l77-057, 1977.

Croce, P.and Formichi, P. and Landi, F.: Extreme Ground Snow Loads in Europe from 1951 to 2100, Climate, 9, 133, https://doi.org/10.3390/cli9090133, 2021.

Dassault Systèmes: Abaqus/Standard. Version 11.2., Tech. rep., Providence, RI: Dassault Systèmes Simulia Corp., 2017.

del Coz Díaz, J., Álvarez Rabanal, F., García Nieto, P., Roces-García, J., and Alonso-Estébanez, A.: Nonlinear buckling and failure analysis of a self-weighted metallic roof with and without skylights by FEM, Engineering Failure Analysis, 26, 65–80, https://doi.org/10.1016/j.engfailanal.2012.07.019, 2012.

Geis, J., Strobel, K., and Liel, A.: Snow-Induced Building Failures, Journal of Performance of Constructed Facilities, 26, 377–388, https://doi.org/10.1061/(ASCE)CF.1943-5509.0000222, 2012.

Geis, J. M.: The Effects of Snow Loading on Lightweight Metal Buildings with Open-Web Steel Joists, Master's thesis, University of Colorado, http://localhost/files/n583xv25x, 2011.

Holický, M. and Sýkora, M.: Failures of Roofs under Snow Load: Causes and Reliability Analysis, American Society of Civil Engineers, pp. 444–453, https://doi.org/10.1061/41082(362)45, 2009.

IPCC: Special Report on the Ocean and Cryosphere in a Changing Climate, [h.-o. portner, d.c. roberts, v. masson-delmotte, p. zhai, m.602 tignor, e. poloczanska, k. mintenbeck, a. alegra, m. nicolai, a. okem, j.603 petzold, b. rama, n.m. weyer (eds.)], 2019.

IPCC: Climate Change 2021: The Physical Science Basis. Contribution of Working Group I to the Sixth Assessment Report of the Intergovernmental Panel on Climate Change, [Masson-Delmotte, V., P. Zhai, A. Pirani, S.L. Connors, C. Péan, S. Berger, N. Caud, Y. Chen, L. Goldfarb, M.I. Gomis, M. Huang, K. Leitzell, E. Lonnoy, J.B.R. Matthews, T.K. Maycock, T. Waterfield, O. Yelekçi, R. Yu, and B. Zhou (eds.)], Cambridge University Press, 2021.

Krentowski, J., Chyzy, T., Dunaj, P., and Dunaj, P.: Delayed catastrophe of a steel roofing structure of a shopping facility, Engineering Failure Analysis, 98, 72–82, https://doi.org/10.1016/j.engfailanal.2019.01.082, 2019.

Le Roux, E., Evin, G., Eckert, N., Blanchet, J., and Morin, S.: Non-stationary extreme value analysis of ground snow loads in the French Alps: a comparison with building standards, Natural Hazards and Earth System Sciences, 20, 2961–2977, https://doi.org/10.5194/nhess-20-2961-2020, 2020.

Marshall, H.-P., Conway, H., and Rasmussen, L.-A.: Snow densification during rain, Cold Regions Science and Technology, pp. 35–41, 1999.

O'Rourke, M. and Downey, C.: Rain-on-Snow Surcharge for Roof Design, Journal of Structural Engineering, 127, 74–79, https://doi.org/10.1061/(ASCE)0733-9445(2001)127:1(74), publisher: American Society of Civil Engineers, 2001.

O'Rourke, M. and Wikoff, J.: Snow-Related Roof Collapse during the winter of 2010-2011: Implications for Building Codes, American Society of Civil Engineers, https://doi.org/10.1061/9780784478240, 2014.

Otsuki, M., Takahashi, T., Saito, Y., Tsutsumi, T., and Hitomitsu, K.: Study on evaluation of roof snow load considering rain-on-snow surcharge: Statistical evaluation of snow cover and precipitation in winter in Japan, in: Snow engineering: recent advances, pp. 166–172, ICSE 2016, 8th International Conference on Snow Engineering, June 14-17, 2016, Nantes, France, 2016.

Otsuki, M., Takahashi, T., Tomabechi, T., Chiba, T., Tsutsumi, T., Kamiishi, I., Kikitsu, H., Iwata, Y., Ishihara, T., and Okuda, Y.: Study on Estimation Method for Surcharge Snow Load Due to Rainfall, Journal of Structural and Construction Engineering (Transactions of AIJ), 82, 1329–1338, https://doi.org/10.3130/aijs.82.1329, 2017.

O'Donnell, F., Tingerthal, J., and White, S.: Estimation of Ground Snow Loads for Low-Latitude, High-Elevation Regions, Journal of Cold Regions Engineering, 34, 04020 008, https://doi.org/10.1061/(ASCE)CR.1943-5495.0000209, 2020.

Piroglu, F. and Ozakgul, K.: Partial collapses experienced for a steel space truss roof structure induced by ice ponds, Engineering Failure Analysis, 60, 155–165, https://doi.org/10.1016/j.engfailanal.2015.11.039, 2016.

Piskoty, G., Wullschleger, L., Loser, R., Herwig, A., Tuchschmid, M., and Terrasi, G.: Failure analysis of a collapsed flat gymnasium roof, Engineering Failure Analysis, 35, 104–113, https://doi.org/10.1016/j.engfailanal.2012.12.006, special issue on ICEFA V- Part 1, 2013.

Ribes, A.and Thao, S., Vautard, R.and Dubuisson, B., Somot, S., Colin, J., Planton, S., and Soubeyroux, J.-M.: Observed increase in extreme daily rainfall in the French Mediterranean, Climate Dynamics, 52, 1095–1114, https://doi.org/10.1007/s00382-018-4179-2, 2019.

Smart, D.: Storm Filomena 8 January 2021, Weather, 76, 98–99, https://doi.org/10.1002/wea.3950, 2021.

Strasser, U.: Snow loads in a changing climate: New risks?, Natural Hazards and Earth System Sciences, 8, https://doi.org/10.5194/nhess-8-1-2008, 2008.

Takahashi, T., Takahiro, C., and Kazuki, N.: Structural damage caused by rain-on-snow load in Japan, in: Snow engineering: recent advances, pp. 173–178, ICSE 2016, 8th International Conference on Snow Engineering, June 14-17, 2016, Nantes, France, 2016.

Tramblay, Y. and Somot, S.: Future evolution of extreme precipitation in the Mediterranean, Climatic Change, 151, 289–302, https://doi.org/10.1007/s10584-018-2300-5, 2018.

Verfaillie, D., Lafaysse, M., Déqué, M., Eckert, N., Lejeune, Y., and Morin, S.: Multi-component ensembles of future meteorological and natural snow conditions for 1500 m altitude in the Chartreuse mountain range, Northern French Alps, The Cryosphere, 12, 1249–1271, https://doi.org/10.5194/tc-12-1249-2018, 2018.

Vidal, J.-P., Martin, E., Franchistéguy, L., Baillon, M., and Soubeyroux, J.-M.: A 50-year high-resolution atmospheric reanalysis over France with the Safran system, International Journal of Climatology, 30, 1627–1644, https://doi.org/10.1002/joc.2003, 2010.

Winter, S. and Kreuzinger, H.: The Bad Reichenhall ice-arena collapse and the necessary consequences for wide span timber structures, in: 10th World Conference on Timber Engineering, vol. 4, pp. 1978–1985, Miyazaki, Japan, 2008.

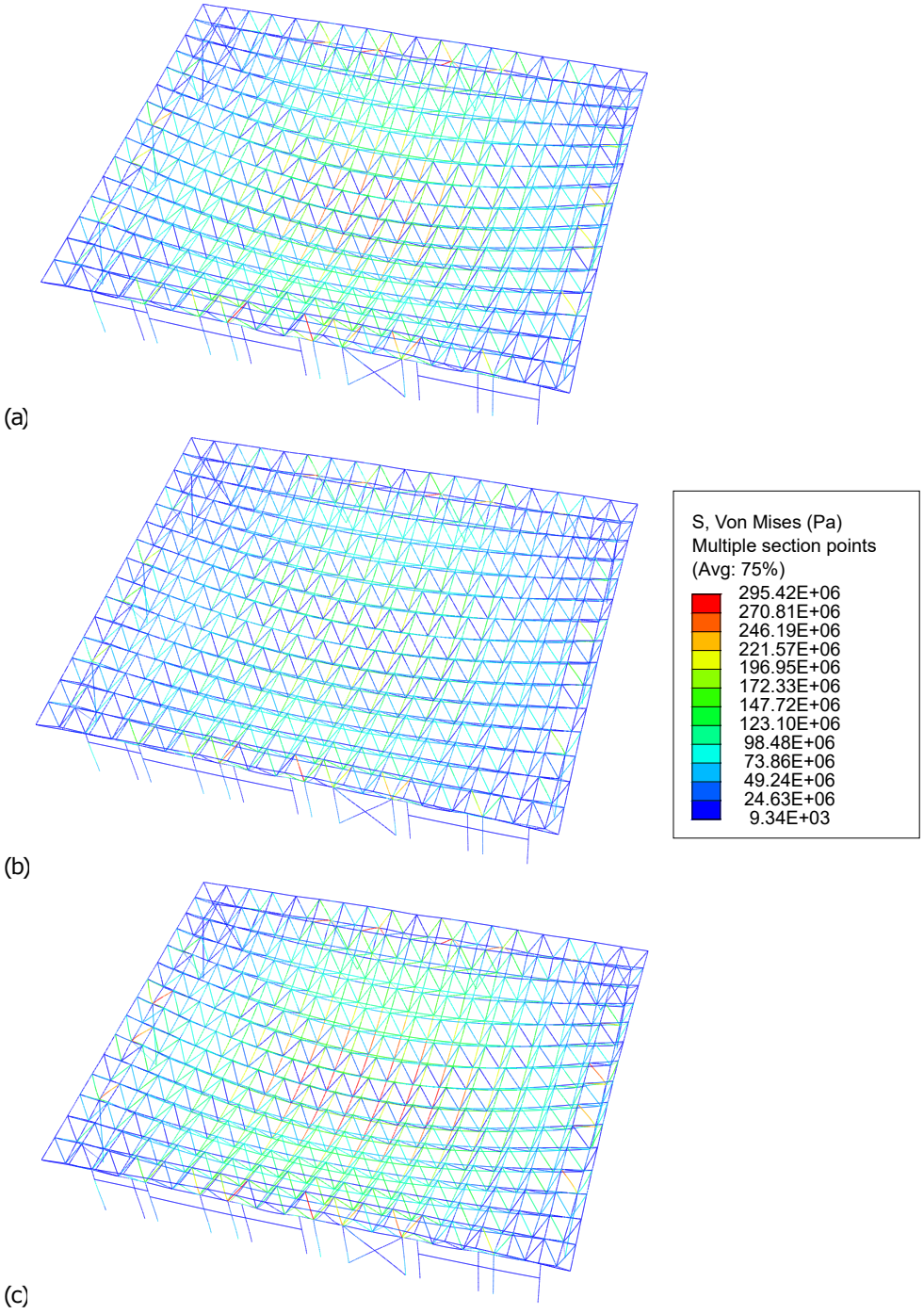

Figure 9. Von Mises stress field (Pa) inside the structure at the real snow-and-rain load of 1 325 $N.m^{-2}$, given by the FE model simulation for the different assumptions made for the spatial distribution of snow and rain: (a) uniform, (b) non-uniform with greater water depth at the edges and (c) non-uniform with greater water depth in the center (a deformation scale factor of 25 is applied to highlight the contrasts).

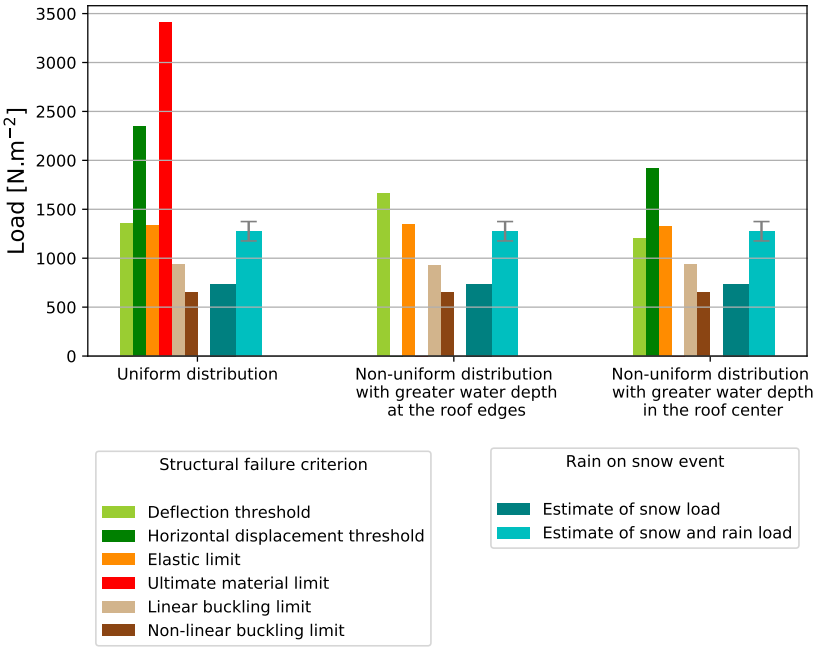

Figure 10. Comparison of the snow loads leading to different failure criteria of the Cévennes building, as calculated by FE model simulations, with ~~different combinations of snow depth and density, assuming a uniform pressure field. The~~ the estimated scenario for the rain-on-snow event of 2018, as back-analyzed in Section 2, in the different cases of snow-and-rain pressure field. The structure fails when the observed snow-and-rain load (on the right, for each assumption of snow-and-rain distribution) is ~~also included~~ greater than a calculated failure load (on the left). The latter calculated failure load could not be obtained when code divergence was observed, thus explaining some empty bars in the ~~comparison~~case of non-uniform rain distributions (see Table 1).